Laboratory assessment of the contribution of aggressive to concrete chemical compounds to the degradation of Portland cement-based materials during anaerobic digestion

Marie Giroudon, Matthieu Peyre Lavigne, Cédric Patapy, Alexandra Bertron

Laboratory assessment of the contribution of aggressive to concrete chemical compounds to the degradation of Portland cement-based materials during anaerobic digestion

Marie Giroudon[1, 2, *], Matthieu Peyre Lavigne [2], Cédric Patapy [1], and Alexandra Bertron[1]

[1] LMDC, Université de Toulouse, UPS, INSA Toulouse, France

[2] TBI, Université de Toulouse, CNRS, INRA, INSA, Toulouse, France

*Corresponding author: marie.giroudon@insa-toulouse.fr

Graphical abstract

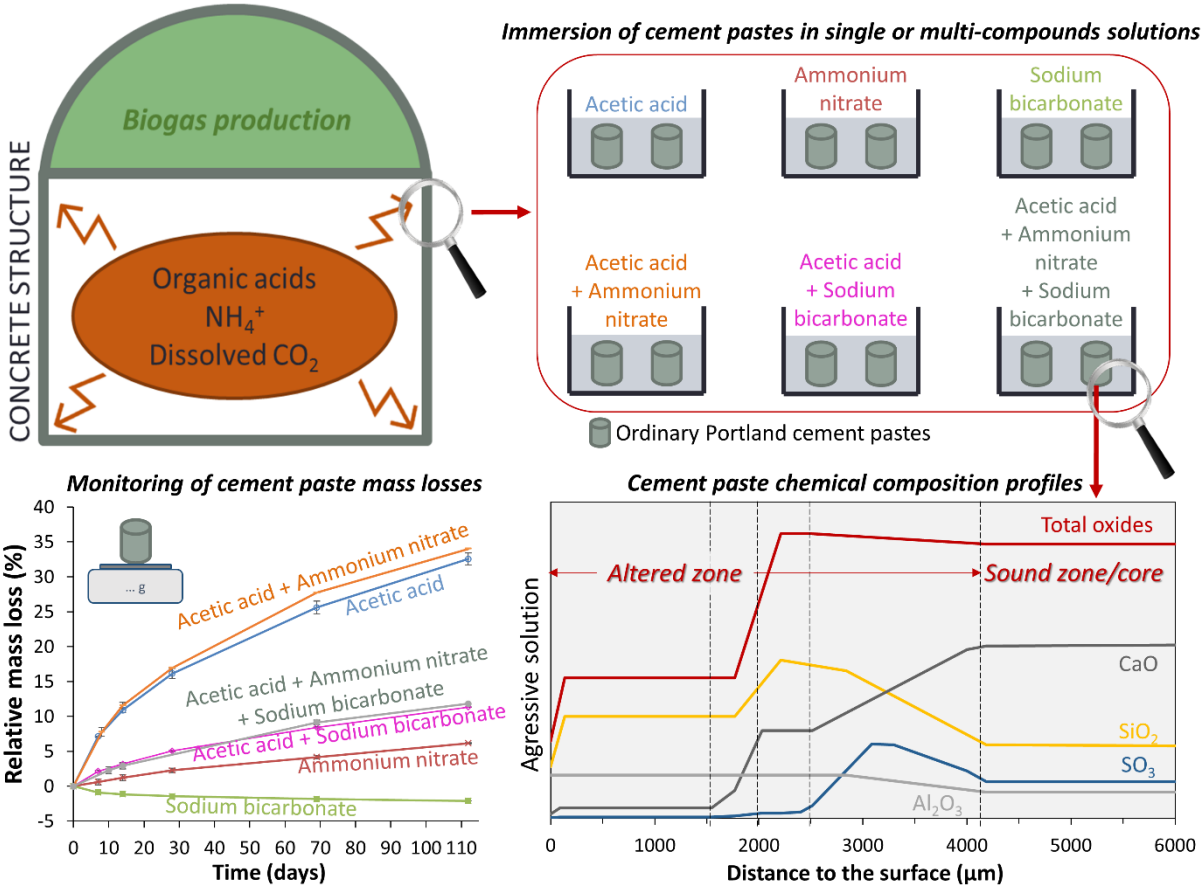

Abstract

Anaerobic digestion allows renewable energy to be produced through the degradation of bio-waste. The process, which is of economic and ecological interest, is implemented industrially in concrete digesters. Bio-waste is a complex medium with a composition that can vary in time and space. It contains several chemical compounds, including volatile fatty acids, ammonium, and CO_2, which are aggressive towards concrete and compromise its durability. The individual effects of the different compounds on concrete are significantly different. To move toward a better design of concrete intended for the building of biogas digesters, this paper aims to understand the mechanisms and intensity of alteration associated with the different components of biowaste and their contribution to the total deterioration. Ordinary Portland cement pastes were immersed for 16 weeks in six synthetic

solutions made of the three metabolites, taken alone or in mixes. The mass variations of the specimens, the pH, and the concentration of the chemical elements in solution were monitored over time. The microstructural, chemical and mineralogical changes of the samples were analysed by scanning electron microscopy, electron probe micro-analysis and X-Ray diffraction analyses and showed phenomena of dissolution, leaching and carbonation. The results show that the acetic acid solution was the most aggressive, in accordance with its pH value, and had a predominant effect in mixed solutions, whereas sodium bicarbonate solution induced carbonation and showed a protective effect. Interestingly, despite its reputed high aggressiveness, ammonium nitrate did not have a major impact in mixed solutions.

Keywords: cement, anaerobic digestion, leaching, acetic acid, ammonium nitrate, sodium bicarbonate

1 Introduction

Anaerobic digestion is a biological process allowing the degradation of organic matter into biogas and digestate by the action of microorganisms. The biogas, mainly composed of methane (CH_4) and carbon dioxide (CO_2) [1–3], can be used in many ways, the most common being cogeneration (75 % of current French installations [4]), which consists of the combined production of heat and electricity. However, France is now turning towards injection into the natural gas network, which allows higher yields [5]. As one of the most environmentally friendly technologies for bioenergy production [6,7], biogas production is supported by the European Union and more than 300 anaerobic digestion plants are being built each year in Europe [8].

Most anaerobic digestion structures are built with concrete because this material is economic, air- and watertight and thermally insulating. The digesters contain two parts: (i) the lower zone (liquid/solid phase) where the successive degradation reactions of hydrolysis, acidogenesis, acetogenesis and methanogenesis [9,10] degrade the biowaste into smaller molecules and (ii) the upper zone containing the biogas produced, and where the walls are generally protected by polymeric liners [11]. In the liquid phase, the digestion of biowaste generates complex and multicomponent environments and deterioration of cementitious materials has been observed in pilot plants and in laboratory tests, in the relatively short term [12–16]. This aggressiveness towards concrete is mainly due to the presence of three chemical compounds, associated with the presence of microorganisms in the form of biofilm: volatile fatty acids (VFA), ammonium cation and dissolved CO_2 are considered to be very aggressive to concrete and their concentrations can vary greatly with time and according to the inoculum and substrate [17,18].

Studies considering the deterioration of cement matrices in fermenting biowaste [13–16] have shown that, for different biowaste/inoculum pairs - and therefore different liquid medium compositions - the intensity and the alteration kinetics are variable, and the degradation is not always a result of the predominant effect of the same metabolite. Although the deterioration induced by each chemical metabolites has been investigated in the literature [19–24], experiments were not necessarily carried out with parameters corresponding to those encountered in the liquid medium of anaerobic digestion (e.g. data is available for very high concentrated ammonium nitrate solutions and atmospheric carbonation). Finally, the individual effects of each aggressive component, and especially their combined effects in the degradation of concrete by the complete medium, are poorly understood.

In this context, this study aims to understand the mechanisms and intensity of alteration associated with the different components of biowaste and their contributions to the total deterioration. It is thus a question of better understanding the deterioration mechanisms in anaerobic digestion structures and reviewing the normative context.

2 Materials and methods

Cement paste specimens made of ordinary Portland cement (OPC) were immersed in six chemically aggressive solutions for 16 weeks. The pH, the mass losses and the concentration of elements in solution were monitored over time. Scanning electron microscopy observations coupled with electron probe micro-analysis, and X-Ray diffraction analyses were used to characterize the chemical and mineralogical changes occurring in the samples.

2.1 OPC paste

There are no precise recommendations on the choice of cement for anaerobic digestion facilities in the normative texts. In agricultural construction in general, other documents issue recommendations to cement such as CEM II or CEM III [25–28]. The choice of cements varies according to the country, without a single, consensual practice being implemented.

Therefore, CEM I-based matrix was used in order to carry out a generic study on the comparative mechanisms and kinetics of attack of different chemical compounds. It should be noted that binders substituted with supplementary cementing materials, containing less portlandite, are more sensitive to carbonation [29–31] whereas OPC are more sensitive to leaching in acidic environments [14,32–34]. This work can be used as a basis for the study of all Portland cement-based matrices such as materials based on CEM II, CEM III, CEM IV and CEM V cements, the use of which is recommended for agricultural constructions [25–28].

CEM I 52.5R (OPC) pastes were made with a water/cement ratio of 0.30 and mixed according to a procedure adapted from the French Standard NF EN 196-1 [35] without adding sand: low speed (140 ± 5 rpm) for 60 seconds and high speed (285 ± 10 rpm) for 90 seconds. This low water/cement ratio was chosen to minimize the porosity and the penetration of aggressive agents into the material. The specimens were cast in cylindrical plastic moulds 70 mm high and 35 mm in diameter, which were closed with plastic caps. After a 28-day endothermic cure and just before the experiment, each cylinder was sawn at half height in order to obtain two cylinders about 35 mm high and 35 mm in diameter. The water porosity of the OPC paste was measured according to the NF P18-459 standard [36] and was 32.0 %.

2.2 Synthetized aggressive solutions

Three single compound-based solutions were prepared: an acetic acid solution representing attack by VFAs (called AA solution), an ammonium nitrate solution representing the attack by ammonium cation (called AN solution) and a sodium bicarbonate solution representing the attack of dissolved CO_2 (called SB solution). An acetic acid solution was chosen to represent the VFA attack since all VFAs (carboxylic acids with less than 5 carbon atoms) have equivalent effects on the cement matrix because their chemical characteristics are similar (pKa and high solubility of their calcium salts) [34,37]. The acid concentration was set to 300 $mmol.L^{-1}$, slightly higher than the value of 280 $mmol.L^{-1}$ used by Bertron et al. [34] and representative of the higher ranges of VFA concentration found in agricultural effluents [38]. For a functional digester, the VFA concentrations can vary from 40 to 250 $mmol.L^{-1}$ [39–41] and these concentrations can exceed 500 $mmol.L^{-1}$ in the case of acidosis [42]. The concentration of the ammonium nitrate solution was chosen according to a previous study of anaerobic digestion in a laboratory set-up [13], where the authors found an ammonium concentration of about 800 $mg.L^{-1}$ and also correspond to the values conventionally encountered in industrial digesters since the concentrations of ammonium ions range between a few hundred $mg.L^{-1}$ and several $g.L^{-1}$ [43,44]. The sodium bicarbonate concentration was chosen in order to represent a gas phase with 50 % of CO_2 (calculated using Henry's law at 35 °C, at atmospheric pressure and for a pH of 7.5), which is slightly higher than the proportion of CO_2 in optimal condition for biogas production [45–47] but which is a

coherent portion with non-optimal conditions for biogas production. Thus, conditions in the high range of aggressiveness were chosen to accentuate the degradation. The solutions were prepared with demineralized water as follows:

- AA solution was a 300 mmol.L^{-1} acetic acid solution (glacial acetic acid 99.8-100.5 %, AnalaR® NORMAPUR – VWR)
- AN solution was a 44.4 mmol.L^{-1} NH_4NO_3 solution (industrial ammonium nitrates, 99.0 % minimum of NH_4NO_3, Orange Label Ammonium Nitrate, MAXAM Tan)
- SB solution was a 243 mmol.L^{-1} $NaHCO_3$ solution (food grade sodium bicarbonate, 99.0-100.5 % $NaHCO_3$, NOVACARB)

Furthermore, solutions combining several chemical compounds together in the same concentrations as above were also studied in order to highlight the contribution of each chemical compound in terms of degradation and aggressiveness mechanisms and to identify combined mechanisms. These solutions were as follows:

- AA+AN solution was a 300 mmol.L^{-1} acetic acid and 44.4 mmol.L^{-1} NH_4NO_3 solution
- AA+SB solution was a 300 mmol.L^{-1} acetic acid and 243 mmol.L^{-1} $NaHCO_3$ solution
- AA+SB+AN solution was a 300 mmol.L^{-1} acetic acid, 243 mmol.L^{-1} $NaHCO_3$ and 44.4 mmol.L^{-1} NH_4NO_3 solution

As the volume of buffer solution to be added was significant (especially in the case of the AA solution), it was chosen not to buffer the solutions, in order to avoid addition of chemical compounds that could possibly interact with the OPC paste.

2.3 Test methods

For each type of solution, four samples were added to 2.5 L which corresponds to a liquid/solid ratio of about 1/17 and a surface area/volume ratio of about 97 $cm^2.L^{-1}$. These values were chosen in accordance with previous studies [34,38,48] to allow comparison. The solutions were kept at 20 °C in closed plastic containers. The pH was measured regularly once the solution was homogenized (daily at the start of the experiment and several times a week thereafter). As soon as the pH of one of the solution exceeded 8.6 (upper limit of anaerobic digestion conditions), a few mL of each solution was sampled for further analyses and all containers were emptied to receive fresh solution. The experiments lasted 16 weeks (112 days). On average, the solutions were renewed every 2.5 (± 1.4) days.

Two of the four samples from the container were dedicated to mass change monitoring and the other two to the microstructural analyses of the materials.

The compositions of the liquid samples were analysed by inductively coupled plasma/optical emission spectroscopy (ICP/OES) (Optima 7000DV ICP/OES Perkin Elmer) (Si, Na, K, Ca, Al, Fe) and high performance ion chromatography HPIC (Dionex ICS-300) (SO_4^{2-}, NH_4^+).

Mass variations were monitored over time: the samples were removed from the solutions, the excess liquid was quickly removed with absorbent paper and, after 5 minutes in the open air, the samples were weighed. After 4 weeks, 10 weeks, and at the end of the experiment, the upper edge of one sample was carefully sawn with a diamond saw and then split in half. One part was used for X-Ray diffraction analysis (XRD) (Brucker D8 Advance, Cu anti-cathode, 40 kV, 40 nA) and the other part was embedded in epoxy resin (Mecaprex Ma2+, Presi) and dry polished using silicon carbide polishing disks (Presi) (polishing disc references and grain sizes: ESCIL, P800–22 µm, P1200–15 µm and P4000–5 µm). The flat polished sections were then coated with carbon and analysed by Electron Probe Micro-Analysis

(EPMA) (Cameca SXFAA+SBe, 15 kV, 20 nA). The chemical composition changes were characterized using chemical profiles, from the surface to the core according to the distance to the surface. Each plotted graph contains values from two experimental profiles in the same specimen. Particular care was taken to analyse hydrated paste and not residual anhydrous grains. The following elements were taken into account in the selection of microprobe: Ca, Si, Al, Fe, S, Mg, Na and K.

To assess mineralogical changes, the plane side of the slice was first analysed, and the sample was then successively abraded and analysed in order to characterize deeper zones, until the sound paste was reached [48].

3 Results

3.1 pH evolution

Figure 1 shows the evolution of the pH of the solutions over time. Each drop in pH corresponds to a renewal of the solutions.

The pH ranges differ quite significantly depending on the nature of the aggressive solution (Figure 1):

- AA and AA+AN solutions have the lowest pH, with fairly strong variations of between 2.4 and 4;
- the AA+SB+AN solution has an intermediate pH range with slight variations (between 4.9 and 5.5);
- the AA+SB solution is the solution showing the smallest variations in pH, since the values are between 5.3 and 5.5, which reflects a strong buffering capacity of the solution;
- unlike the other solutions, the AN solution exhibits strong variations in pH, between 5.6 and 9, reflecting the low buffering capacity of this solution;
- the SB solution has the highest initial pH and the pH variations are between 8.2 and 9.

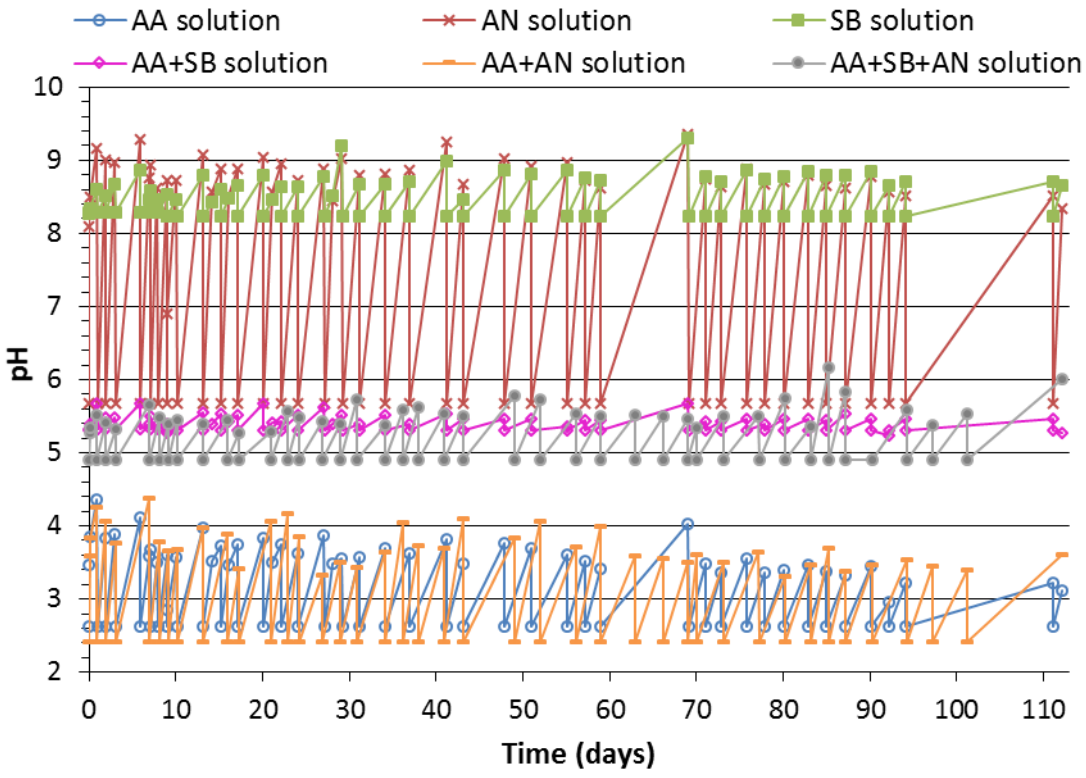

Figure 1: pH evolution of the solutions according to time of immersion (AA: acetic acid, AN: ammonium nitrate, SB: sodium bicarbonate)

3.2 Total leaching of chemical elements in the solutions

Table 1 brings together the cumulative mass of elements leached in solution, per sample, at the end of the experiment. The cumulated concentrations and leaching kinetics are given as supplementary data (Appendix A).

*Table 1: Cumulative leached ions per cement paste sample in the solutions during the experiment (AA: acetic acid, AN: ammonium nitrate, SB: sodium bicarbonate). *concentrations cannot be provided with sufficient precision, see text.*

	Cumulative leached ion from the specimens (mmol)						
	Calcium	Silicon	Aluminium	Sulfate	Iron	Potassium	Sodium
AA solution	423 ± 46	15.6 ± 1.7	9.1 ± 1	2.2 ± 0.2	3.5 ± 0.4	7.1 ± 0.8	2.9 ± 0.3
AN solution	166 ± 18	5.1 ± 0.6	0.0 ± 0	0.5 ± 0.1	0.0 ± 0	5.3 ± 0.6	2.1 ± 0.2
SB solution	0.0 ± 0	1.2 ± 0.1	0.0 ± 0	0.0 ± 0	0.0 ± 0	4.1 ± 0.4	-*
AA+AN solution	415 ± 46	17.8 ± 2	9.0 ± 1	0.8 ± 0.1	3.1± 0.3	7.8 ± 0.9	7.8 ± 0.9
AA+SB solution	137 ± 15	3.2 ± 0.3	0.0 ± 0	1.7 ± 0.2	0.0	5.0 ± 0.6	-*
AA+SB+AN solution	185 ± 20	5.4 ± 0.6	0.0 ± 0	0.6 ± 0.1	0.0	6.9 ± 0.8	-*

It was not possible to precisely quantify the variations of sodium concentration in SB, AA+SB and AA+SB+AN solutions since the concentrations of sodium were originally very high in solution, and the variations in the measured concentrations were not large enough to be significant.

Solutions containing acetic acid and no sodium bicarbonate, i.e. AA and AA+AN, were the most aggressive in terms of leaching, with slightly lower amounts measured for the AA+AN solution compared to the AA one: in both solutions, greater amounts of calcium (mean value of the two samples of about 419 ± 5.1 mmol), silicon (17 ± 1.6 mmol) and sulfates (2 ± 0.3 mmol) were found. Moreover, these solutions were the only ones to generate aluminium (9 ± 0.1 mmol) and iron (3 ± 0.3 mmol) leaching, which might be related to their low pH. The decreasing order of ion release in both solutions was as follows: Ca^{2+}> Si^{4+}> Al^{3+}> K^{+}> Fe^{3+}> SO_4^{2-}.

Solutions of ammonium nitrate AN, and acetic acid containing bicarbonate with or without ammonium nitrate, AA+SB and AA+SB+AN, were less aggressive and showed intermediate leaching values for calcium (163 ± 25 mmol), silicon (5 ± 1.2 mmol), sulfates (1 ± 0.1 mmol), and potassium (1 ± 1.2 mmol). These solutions did not lead to iron and aluminium leaching within the duration of the experiment. The decreasing order of ion release in both solutions was as follows: Ca^{2+} > Si^{4+} > SO_4^{2-} and K^{+}.

Sodium bicarbonate solution SB was the least aggressive and only small amounts of potassium (4.1 mmol) and silicon (1.2 mmol) were released. There is therefore a relative release of the ions as follows: K^{+} > Si^{4+}.

3.3 Macroscopic observations of specimens

Figure 2 shows the macroscopic aspects of the samples at the end of the immersion experiments.

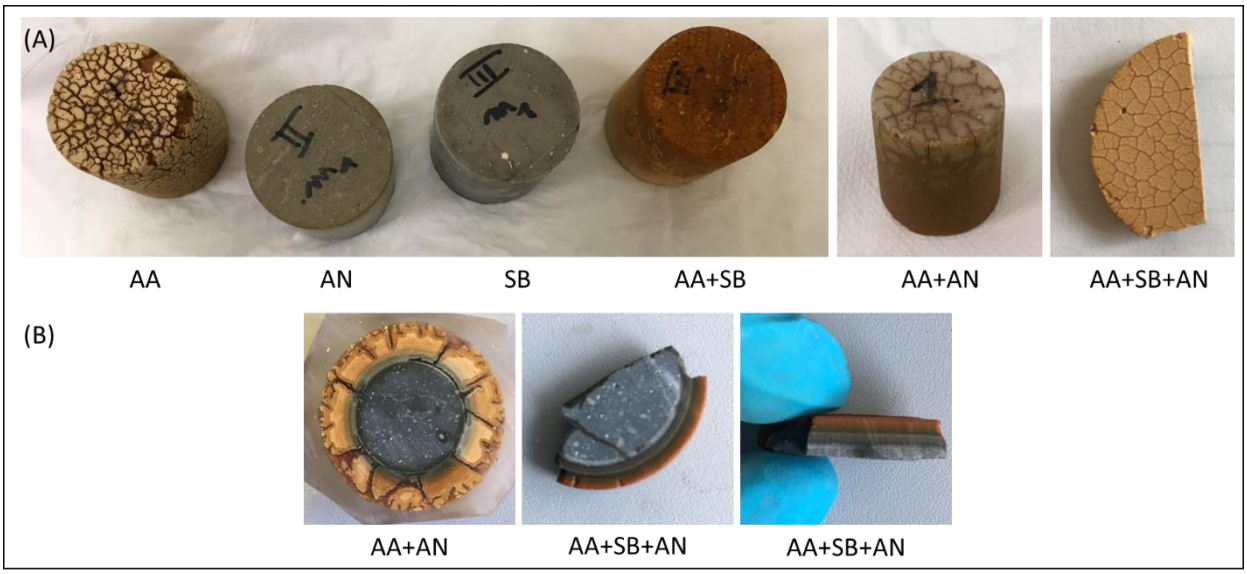

Figure 2: (A) Visual appearance of the samples' surfaces at the end of the experiment and (B) visual appearance of the slices of the samples AA+AN and AA+SB+AN at the end of the experiment (AA: acetic acid, AN: ammonium nitrate, SB: sodium bicarbonate)

Samples immersed in solutions containing acetic acid (AA, AA+SB and AA+SB+AN) showed an orange colour because the intense decalcification of the cement matrix allowed the expression of the iron oxide colour. For the AA, AA+SB and AA+SB+AN solutions, a dense crack network was observed when these samples were taken out of the solutions and left to dry on a bench. This cracking was related to chemical shrinkage as a result of calcium being leached from the sample in large quantities. Figure 2 shows that the coloured zonation is a function of the distance to the exposed surface. Finally, the colour is preserved for the cement paste exposed to the sodium bicarbonate (SB) solution, whereas the sample immersed in the ammonium nitrate (AN) solution shows a slight orange colouring, without cracking.

3.4 Microstructural observations

Figure 3 shows the SEM images of the OPC samples after 4 weeks or 10 weeks of immersion in the aggressive solutions and at the end of the experiment (16 weeks). Since the samples immersed in the SB solution did not show any significant changes, the SEM images are only shown for 10 weeks and 16 weeks. Moreover, it should be noted that, on the same sample, the difference in density between the degraded zone and the sound core was sometimes so great that the two zones could not be correctly observed with the same contrast. Some of the images presented are therefore an assembly of two images with different contrasts.

AA solution

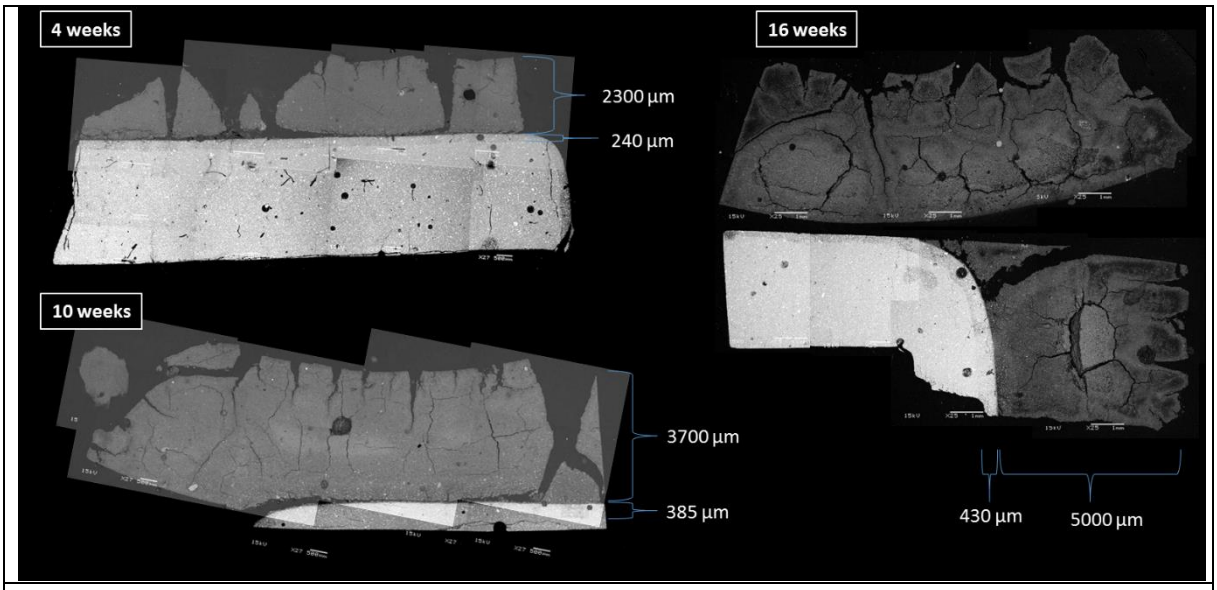

AN solution

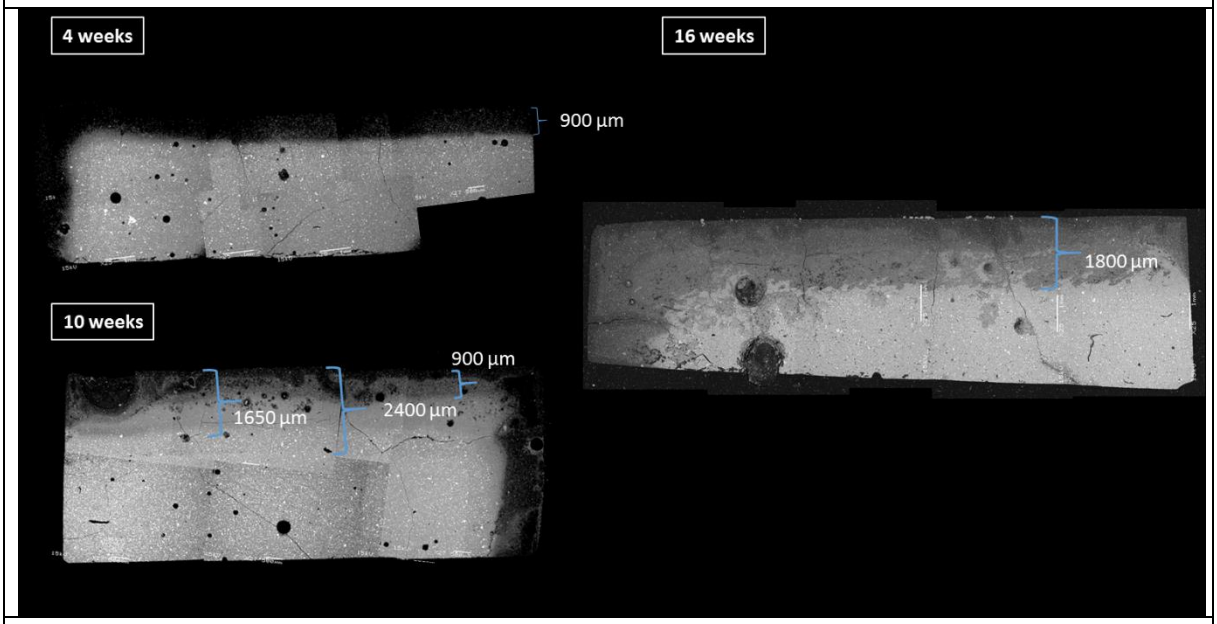

SB solution

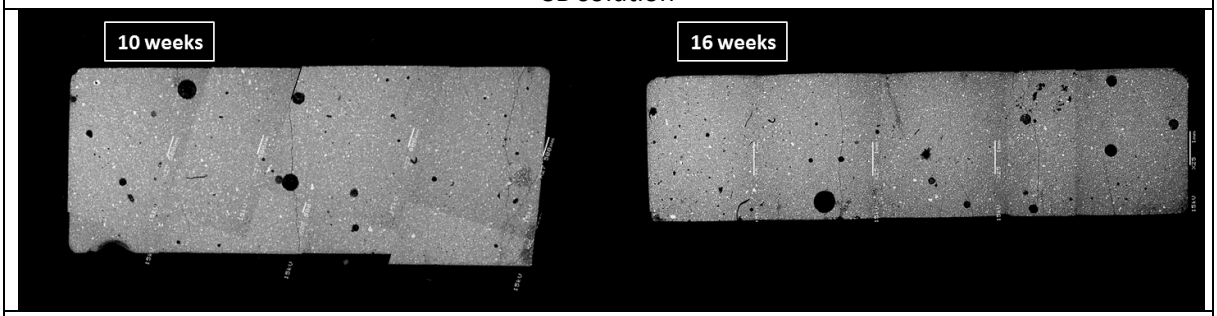

AA+AN solution

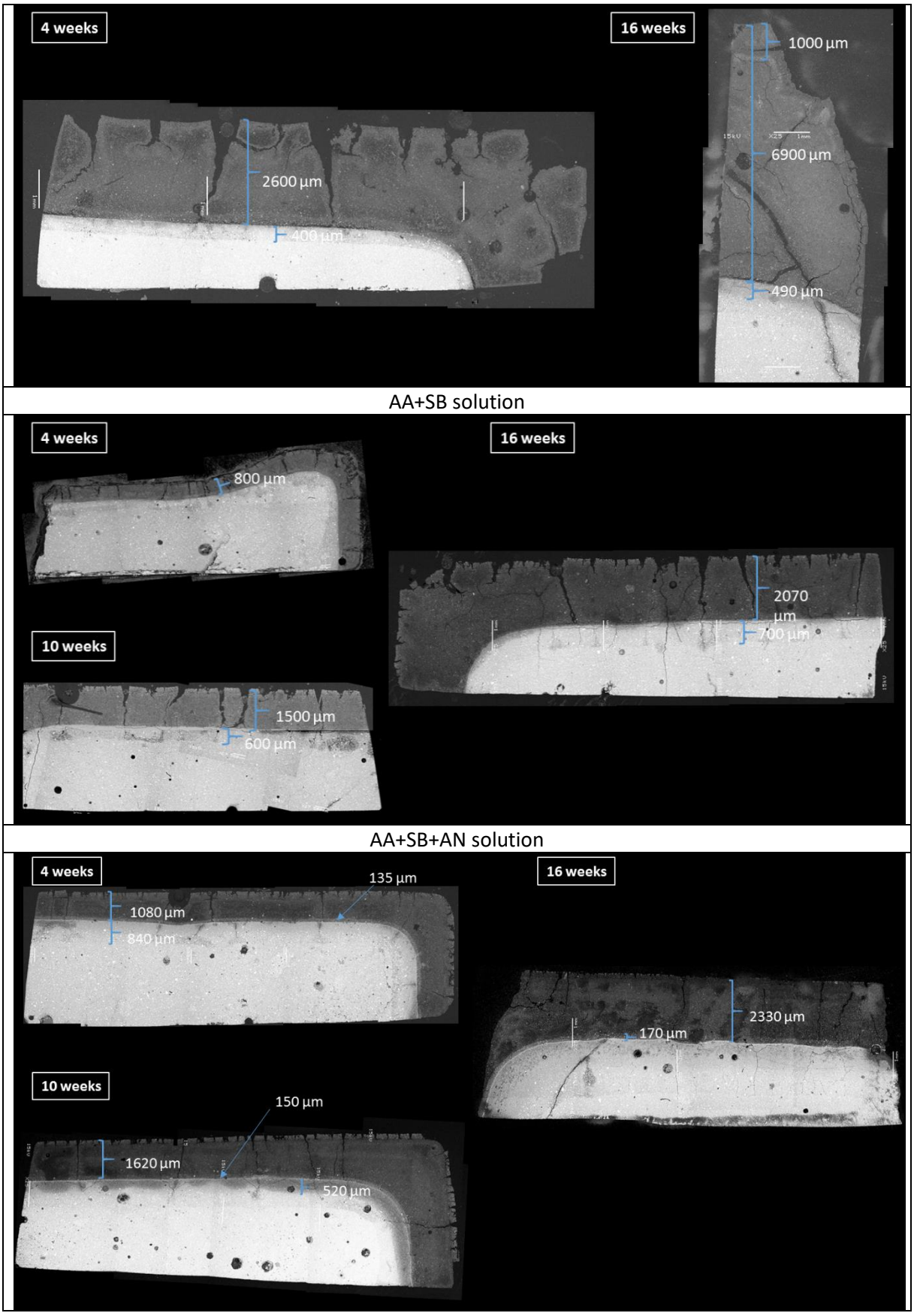

Figure 3: SEM images of OPC paste samples immersed in the different aggressive solutions after 4 weeks, 10 weeks and 16 weeks (AA: acetic acid, AN: ammonium nitrate, SB: sodium bicarbonate). Approximate magnification: x25. Some of the images are an assembly of two images with different contrasts.

From the macroscopic and microscopic observations, three types of microstructural patterns can be observed:

- In the presence of acetic acid, the samples show an outer degraded zone (hereafter called the degraded zone) of very low density, yellowish to brownish in colour (Figure 2), friable and subject to desiccation shrinkage for the samples removed from the bins and dried before observation (very porous zone) (see Figure 2, samples AA, AA+SB, AA+AN and AA+SB+AN). The cracking observed on wet samples is related to the chemical shrinkage associated with the departure of the ions. This area has a completely different structure from the sound paste: the anhydrous grains are no longer visible and it has very low mechanical strength, as pointed out by several authors in studies on acetic, lactic or succinic acids [33,34,49]. Below the degraded zone, a thinner area appears, slightly darker than the sound core, and therefore slightly less dense. In this area, anhydrous cement grains can still be observed. The limits between the different zones are clear and the fronts are parallel to the surface. The degraded zone tends to detach from the rest of the sample when dry.
- Samples exposed to the AN solution show an outer zone of lower density, with a non-rectilinear limit between the sound core and the zone of lower density. The attack by AN being much less aggressive than that of acetic acid, the diffusive phenomena might take a higher part in the deterioration pattern compared to acid attack that creates a sharp front of cementitious matrix dissolution. The heterogeneous microstructure of the cement matrix in terms of pores, air voids and microcracks provides preferential routes for the ingress of the AN solution, leading to this irregular deterioration front.
- For samples exposed to the SB solution, no change is clearly visible on the SEM images, whether after 4, 10 or 16 weeks. However, an intensification of the calcium signal could be seen on the surface on the EDS maps (not shown here).

On samples exposed to both acetic acid and sodium bicarbonate (AA+SB and AA+SB+AN), there is a thin cracked outer layer with a slightly higher density than that of the degraded part just below.

3.5 Mass variations and degraded layer depths

Figure 4 shows the evolution of the mass variations of the OPC paste in the different solutions and Figure 5 the degraded layer depths, obtained from the SEM observations presented in Figure 3. After 112 days of immersion, the OPC paste is seen to have undergone a significant mass loss of about 33 % for the AA and AA+AN solutions, with a slightly more severe attack for the AA+AN solution. Conversely, a mass gain of 2.1 % is observed when the OPC paste is immersed in the bicarbonate sodium solution. The other solutions have an intermediate aggressiveness. The lowest mass losses (6.1 %) are observed for the AN solution (ammonium nitrate only) whereas the immersion in the AA+SB and AA+SB+AN solutions leads to similar higher mass losses of about 11.5 % at the end of the experiment. Based on these results, it is observed that ammonium nitrate is much less aggressive to the cement matrix than acetic acid is, and sodium bicarbonate appears to provide a protective effect when it is present in solution with acetic and/or ammonium nitrate. In mixtures, the additional effect of ammonium nitrate in terms of aggressiveness appears almost negligible. It can be noted that the mass variation classification is unsurprisingly consistent with the pH of the solutions (Figure 1): the AA and AA+AN solutions have identical pH values and mass losses and the same is true for the AA+SB and AA+SB+AN solutions. The AN and SB solutions are those exhibiting the highest pH and the lowest mass losses. Beyond the aggressiveness of the metabolites, there is therefore also an effect of acidity on degradation.

In all the solutions, the mass loss kinetics are higher in the first weeks, and tend to slow over time. This could be due to the slowing down of the penetration of aggressive agents into the cement matrix

because of the greater depth of paste to cross (diffusion). It can also be noted that, in view of the cylindrical geometry of the samples, a smaller and smaller volume of paste is degraded as the aggressive agents penetrate.

Except for the AN solution, for which it is difficult to precisely identify the different areas of degradation and their evolution (see Table 1), there is a clear increase in the thickness of the degraded area over time, with a similar evolution for the AA and AA+AN solutions and for the AA+SB and AA+SB+AN solutions. This evolution is correlated with the mass losses shown in Figure 4, and with the pH. The aggressive trend shown by the mass losses is confirmed since, at the end of the experiment, the degraded depths (measured with SEM images) reached thicknesses of 0 µm, 1800 µm, 2070 µm, 2330 µm, 5000 µm and 6900 µm respectively for the SB, AN, AA+SB, AA+SB+AN, AA and AA+AN solutions. It is interesting to note that the deteriorated layer thicknesses of cement pastes exposed to solutions containing AN, AA + AN and AN, are relatively larger than those observed in other solutions when their relative aggressiveness in terms of mass losses is considered.

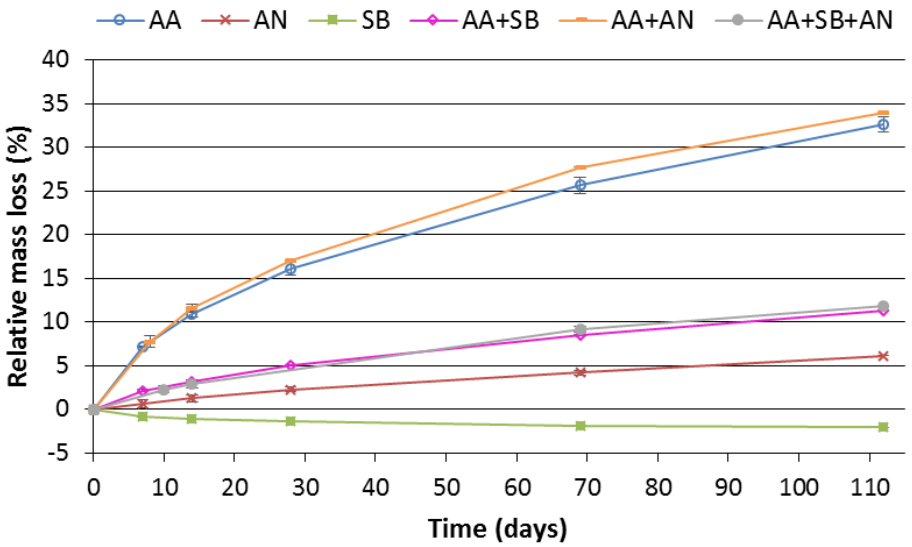

Figure 4: Mass losses of the OPC paste according to the time of immersion in the aggressive solutions (AA: acetic acid, AN: ammonium nitrate, SB: sodium bicarbonate)

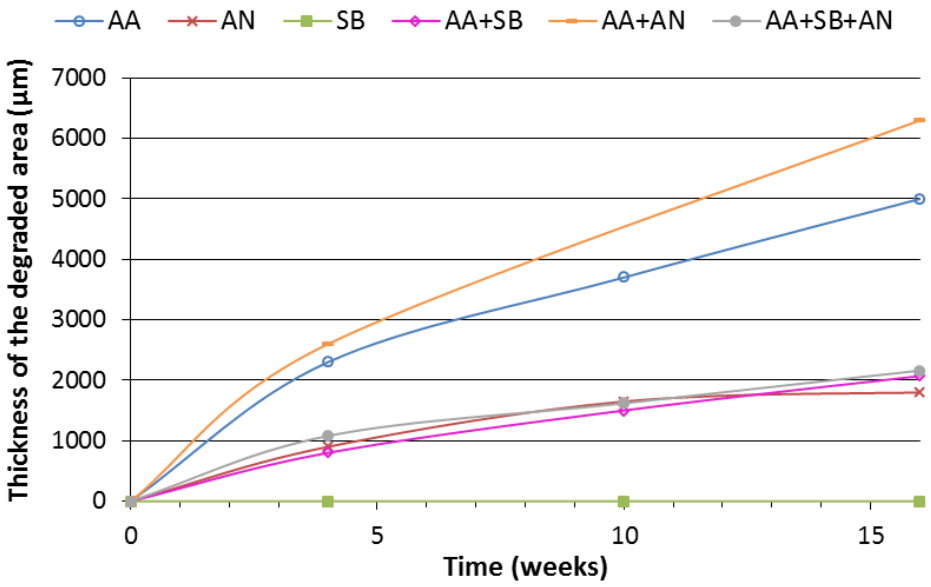

Figure 5: Evolution of the degraded depth of the samples (from SEM observations) over time according to the aggressive solution (AA: acetic acid, AN: ammonium nitrate, SB: sodium bicarbonate)

3.6 Chemical and mineralogical changes

Figure 6 shows the major chemical and mineralogical changes in the OPC pastes immersed in the synthetic solutions for 16 weeks. The data are given in amounts of oxides according to the distance to the surface. Thus, the sum of all the oxide amounts (Total) gives indications about the deterioration of the cement paste. For greater clarity, the profiles of chemical compositions were modelled and only the main trends are represented. The original plots are given as supplementary data (Appendix B). The main patterns of the mineralogical analysis by XRD obtained at different depths by successive abrasion of the degraded surface have been added on the same figure. The original diffractograms of the samples immersed in the AA, AN and SB solutions are given as supplementary data (Appendix C, Appendix D and Appendix E). The chemical and mineralogical zonation is represented on the graphs. The core of the specimens with the same composition as the unexposed control specimens is noted zone 1 for all the materials.

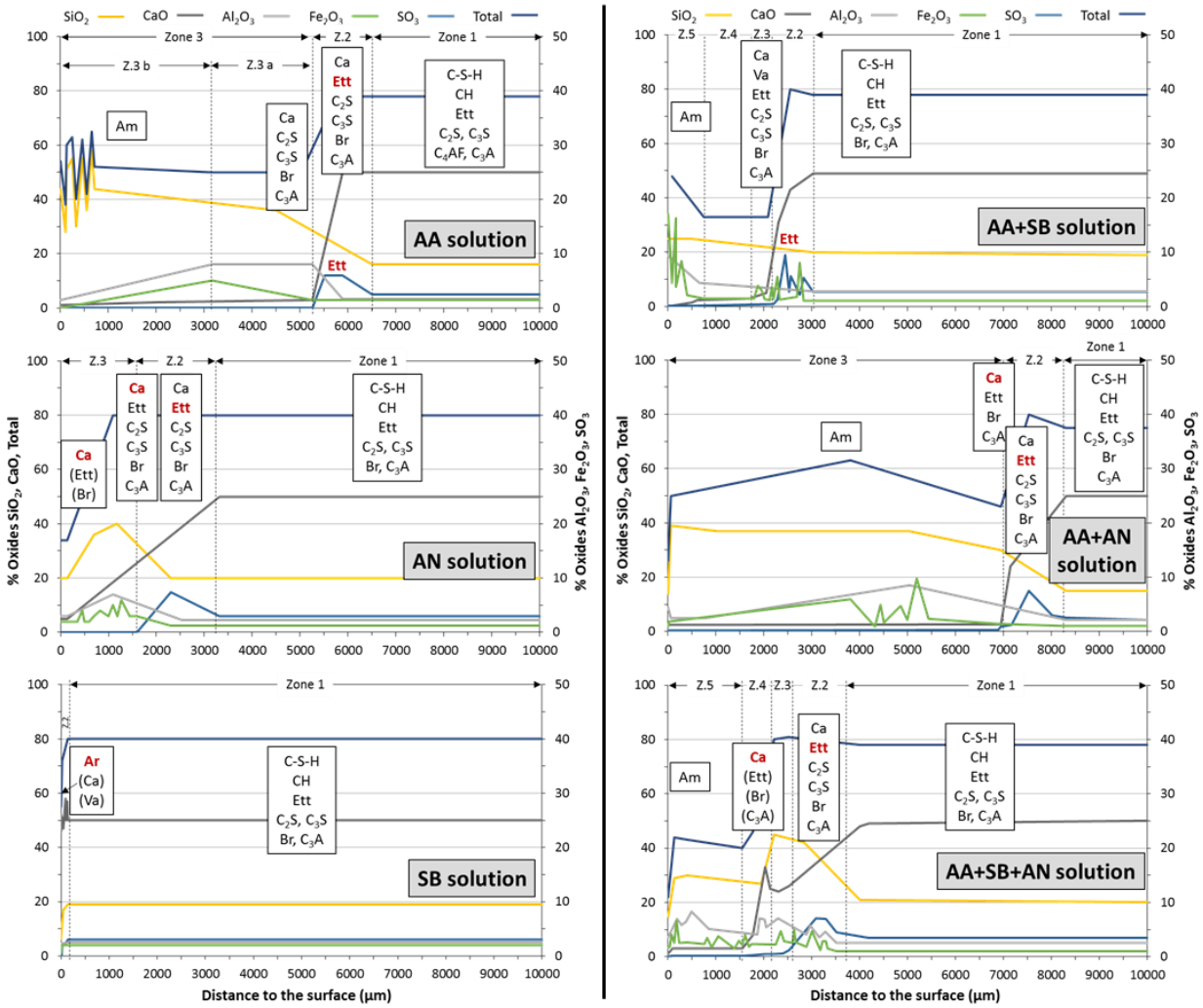

Figure 6: Schematic representations of chemical composition of oxides and mineralogical composition (analysed by EPMA and XRD, respectively) of the OPC pastes after 16 weeks of immersion in the aggressive chemical solutions (AA: acetic acid, AN: ammonium nitrate, SB: sodium bicarbonate) – Ett: ettringite; Ca: calcite; Va: vaterite; Br: brownmillerite; Am: mainly amorphous pattern – Red bold characters = intensification of the XRD signal in comparison with the deeper zone; Parentheses = significantly lower intensity of the XRD signal in comparison with the main phase

3.6.1 AA solution

Zone 1 (the sound zone) contains typical phases of a Portland paste (portlandite, ettringite, brownmillerite, C_3A[1], C_3S and C_2S). The EPMA chemical analysis shows a thick degraded zone of 6400 µm (zone 2 + zone 3) with a total and sharp decalcification of the paste occurring in zone 2. From a mineralogical point of view, this zone shows the dissolution of the portlandite and the precipitation of calcite. A slight enrichment in ettringite may be associated with the increase of the sulfur content. Zone 3 shows an amorphization of the paste, with a predominantly amorphous outer zone more than 4 mm thick. It consists of an amorphous aluminium-silicate skeleton containing iron: in zone 3.a, the aluminium, iron and silicon contents show a relative increase due to the significant decrease in the calcium content and there is then a gradual decrease in aluminium and iron in zone 3.b. The outer surface is made of silica gel only.

[1] Cement chemistry shorthand notations: A = Al_2O_3, C = CaO, F = Fe_2O_3, H = H_2O, M = MgO, S = SiO_2

3.6.2 AN solution

Beyond 3100 µm (zone 1), the paste seems unaltered, with a chemical composition corresponding to a sound OPC paste. The EPMA chemical analysis shows a very gradual decalcification from 3100 µm depth (start of zone 2) with no sharp drop in the calcium content, reflecting a less aggressive attack than for the AA solution. Zone 2 is characterized by the dissolution of portlandite and an enrichment in sulfur content, associated with the intensification of the ettringite peaks. Calcite precipitation is detected. From 2500 µm, the SiO_2, Al_2O_3 and Fe_2O_3 contents increase whereas the sulfur content decreases. The SO_3 content reaches 0 % in zone 3 and the SiO_2 content and the total oxides content decrease from 1150 µm onwards. The paste chemical composition is stable over the last 100 µm, where only the brownmillerite phase and some ettringite remain from the initial composition of the OPC paste, and calcite is the main phase (zone 3).

3.6.3 SB solution

The chemical composition of the OPC paste immersed in SB solution changed very little after 16 weeks of immersion. Only a thin external layer about 50 µm thick (zone 2) shows changes, with a decrease in the total oxides content (from 80 % to 55 %) as well as a decrease in each oxide content except for calcium oxide, which remains around 50 %. The stable calcium content is might be due to the phenomena of dissolution and precipitation of calcium carbonates, since the only detected phases of the outer layer are carbonation products: mainly aragonite, but also calcite and vaterite

3.6.4 AA+AN solution

The specimen in the AA+AN solutions shows the greatest degraded depth, significantly greater than in AA, contrary to what the mass loss suggested. The chemical changes are similar to those of the specimen in the AA solution but with a greater degraded depth. Decalcification occurs in zone 2: it starts from 8100 µm depth and is complete at 7000 µm depth. This decalcification is less sharp than in AA solution and extends over more than a millimetre, as for the immersion in AN solution, while the drop in the total oxide content occurs suddenly at a depth of about 7000 µm. As for other solutions containing acetic acid, a sulfur enrichment associated with the intensification of the ettringite X-ray diffraction peaks is observed in zone 2, just before this element is completely leached out. The total oxides content drops from 80 % to 40 % between 7200 and 6800 µm. Then, zone 3 is made of Al_2O_3, Fe_2O_3 and SiO_2 up to 1000 µm deep but only SiO_2 remains on the surface.

3.6.5 AA+SB solution

The EPMA analysis of the OPC paste immersed in AA+SB solution shows a chemical composition similar to that resulting from the acetic acid attack, with a smaller degraded depth than for the AA solution. Zone 2 shows a sudden drop in calcium oxide as well as total oxides and sulfur enrichment. It is marked by the dissolution of portlandite and the intensification of the ettringite peaks. Calcium carbonates, calcite and vaterite, are detected. There is no longer any SO_3 in zone 3 but the paste is not completely decalcified, which could be linked to the precipitation of calcium-rich phases in this zone. The mineralogical analysis shows the dissolution of the initial phases of the paste in favour of calcium carbonate, calcite and vaterite, for which intensity of the peaks increases. In zone 4, the cement matrix is decalcified, with a total oxide content of less than 40 %. In this solution, compared with the AA solution, the aluminium and iron oxides are better preserved in the outer layer, resulting in a smaller relative increase in the silica content. As for the AA solution, the outer zone (zone 4) is completely amorphous and the surface is composed of a Si-Fe-Al gel. The increase in the total oxide content is observed in the outer 400 µm due to the increase in the Fe_2O_3 content.

3.6.6 AA+SB+AN solution

The EPMA chemical analyses of the OPC paste immersed in AA+SB+AN solution show a progressive decalcification (as for AN solution) from 3500 to 2100 µm (zones 2 and 3) and a sharper decalcification

(as for AA solution) from 2000 µm to 1750 µm. Zone 2 shows an enrichment in the SO_3 content associated with more intense ettringite peaks in the XRD analysis. Zone 3 is marked by the stabilization of the calcium content, probably due to the precipitation of calcium carbonates (main phases detected by DRX analyses). This induces a high total oxides content, an effect that is much more significant in this solution, in the presence of AN, than for the AA+SB solution. Zone 4 shows the decrease of the SiO_2 and CaO contents, associated with the drop of the total oxides content. The external layer (zone 5) is made of an Si-Al gel. The external layer of this specimen is mainly amorphous but weak peaks of brownmillerite are detected.

4 Discussion

4.1 Phenomenology

According to the mass losses and the degraded depths identified in the EPMA analyses, the solutions studied in these conditions can be classified in increasing order of aggressiveness (considering the modified depth): SB solution < AN solution < AA+SB solution < AA+SB+AN solution < AA solution < AA+AN.

4.1.1 Degradation by acetic acid alone

The degradation mechanisms of the OPC paste immersed in AA solution were those classically encountered in acid attacks for acids whose calcium salts are soluble in water [37]:

- A progressive dissolution of all the initial phases of the cement paste
- Significant mass losses
- A degraded area almost totally decalcified and made of aluminium, silicon and iron. This completely amorphous structure was similar to that of a silica gel and / or a silico-aluminous gel.

Moreover, as in the study by Bertron et al. [48], a slight sulfur enrichment was observed just in the transition zone between the amorphous outer zone and the sound zone, corresponding to the intensification of the ettringite peaks.

Calcium and sulfates were the most leached elements (Table 1), and were not found in the amorphous outer layer (Figure 6).

As in the study by Bertron et al. [48], the altered zone had weaker mechanical strength but was not dissolved and could have slowed down the ingress of aggressive agents into the core of the sample.

4.1.2 Degradation by ammonium nitrate alone

According to the literature [22,50], ammonium salts are aggressive for the cement matrix and react according to an exchange mechanisms $2\ NH_4^+ \rightarrow Ca^{2+}$, leading to the leaching and decalcification of the cementitious matrix [24], the degradation being governed by diffusion [23]. Highly concentrated ammonium nitrate solutions (6 $mol.L^{-1}$ or more) are thus used to provide accelerated tests of pure water leaching [21,51–53]. Both pure water and ammonium nitrate solution lead to the total dissolution of portlandite and the decalcification of C-S-H, and to a sulfur enrichment in the degraded area, the difference being that the kinetics of the degradation in the ammonium nitrate solution are 60 to 300 times higher than in deionized water [51,54–56]. The ammonium nitrate solution attack creates an external degraded zone [21,52,53] and induces a significant increase in the porosity [23,52]. Moreover, the C/S of the C–S–H decreases and the porosity and the diffusivity increase when the NH_4NO_3 concentration in the immersion solution is increased [57,58].

In this study, a low concentration of ammonium nitrate solution was used (4.44 mmol.L^{-1}) in order to reproduce the anaerobic digestion conditions. In this context, the ammonium nitrate attack resulted in the progressive decalcification of the paste with the dissolution of the Ca-bearing phases (CH and C-S-H) and led to surface carbonation. The carbonation might be due to the presence of dissolved CO_2 (from the air) in solution. It probably slowed down the progression of the attack by clogging the porosity [59,60]. As for AA solution, sulfates and calcium were the most leached elements but they were in lower concentrations. However, the amount leached out was lower than for the AA solution, which is consistent with the smaller degraded depths and mass losses of these samples, as well as the decalcification - which was only progressive in the degraded zone, whereas it was total over the entire area for the AA solution. Unlike during the acid attack, the iron remained in the outer layer.

4.1.3 Degradation by the sodium bicarbonate alone

After 16 weeks, the OPC paste immersed in sodium bicarbonate solution remained intact except in a thin outer layer composed only of carbonation products: calcite, vaterite and aragonite. These samples were the only ones to show mass gains, linked to the carbonation layer deposited on the surface. Above a pH of 8, when the pH increases, the equilibrium of bicarbonate to carbonate ions is shifted towards carbonate (pKa1 (H_2CO_3/HCO_3^-) = 6.30; pKa2 (HCO_3^-/CO_3^{2-}) = 10.33). In the sodium bicarbonate solution, the pH was between 8 and 9 during the experiment (Figure 1) and was certainly higher in contact with the OPC paste. Thus, the carbonate ions in contact with $Ca(OH)_2$ led to calcium carbonates precipitation. Among the elements analysed, only silicon and potassium were leached in small amount. It can be noted that the amount of leached potassium was lower than in the other solutions, whereas in the other solutions this element was leached in similar quantities, whatever the solution aggressiveness. Thus, it seems that the sodium bicarbonate solution limits the leaching by clogging the porosity with calcium carbonates [59,60]. Whereas calcite is known to be the most stable polymorph of calcium carbonates under ambient atmospheric conditions [61], the external layer of the paste was mainly made of aragonite (metastable phase) and also contained vaterite (unstable phase) in small amounts (solubility product at 25°C: logK_{sp}= -8.48, -8.34 and -7.91; molar volume: 35 $cm^3.mol^{-1}$, 34 $cm^3.mol^{-1}$ and 38 $cm^3.mol^{-1}$ for calcite, aragonite and vaterite, respectively [62,63]). According to several authors [64–66], the Na^+ ion has no effect on the polymorph formed. However, pure aragonite phases can be synthesized by adding sodium carbonate Na_2CO_3 to a $Ca(OH)_2$ solution in controlled conditions [67,68]. According to Kitamura et al. [68], the aragonite content increases when the addition rate of sodium carbonate decreases, and for a high addition rate, calcite preferably precipitates. The authors specify that, if the concentration of calcium ions is at or near the solubility of $Ca(OH)_2$, the low local supersaturation of carbonate ion is advantageous for the crystallization of aragonite. This phenomenon could explain the presence of aragonite in the external layer of the paste. Furthermore, the presence of vaterite may be related to the lower pH of the external layer, since, at ambient temperature, vaterite precipitates for pH<10 [69,70].

The formation of calcium carbonates, reflecting the carbonation phenomenon, is known to be a major risk of corrosion in reinforced concrete, by depassivation of reinforcements [71]. Moreover, the carbonation phenomenon could be even more detrimental for concrete with blended cement: the use of supplementary materials leads to a decrease in the portlandite content for the benefit of C-S-H, whereas the carbonation of C-S-H results in significant shrinkage, loss of cohesion, increase in the number of pores and increased porosity [72–75].

4.1.4 Degradation by the combined solutions

Acetic acid combined with the other aggressive compounds

The degradation mechanisms of the cement paste immersed in the AA+AN, AA+SB and AA+AN+SB solutions can be explained by the combination of the degradation phenomena caused by the aggressive agents in solution but the intensity and kinetics of the attack are mainly related to the AA attack. The structural degradations and the chemical composition profile of these cement pastes are similar to those of the cement paste immersed in the AA solution, although differences can be noted: acetic acid leads to the leaching of all the elements, significant mass losses and degraded depths.

Ammonium nitrate combined with the other aggressive compounds

In the AA+AN and AA+SB+AN solutions, the presence of ammonium nitrate increased the degraded depths and intensified the degradations, but in a moderate way with a relative increase in mass loss of 4% and of 24 % in degraded depth for the AA+AN solution compared to the AA solution. In the AA+AN solution, a sudden decalcification was observed as for an acid attack, combined with a more gradual decalcification in depth, probably linked to the presence of ammonium nitrate. The quantities of elements released in this solution were similar to those in AA solution, except for sodium and sulfates: it appears that the presence of ammonium nitrate accentuates the sodium leaching and the global degradation, while limiting the sulfates leaching.

For the AA+SB+AN solution, despite the periodic renewals of the solution, which is the most influential factor for the aggressiveness of an ammonium nitrate solution of given concentration [76], the presence of ammonium nitrate in such concentration did not seem to significantly increase the degradation. If we compare the degradation of the cement paste immersed in the AA+SB solution and that immersed in the AA+SB+AN solution, it can be observed that the presence of ammonium nitrate increased the mass loss of the sample only slightly: in the presence of ammonium nitrate, some elements were more leached (calcium, potassium and silicon) and it was again observed that the leaching of sulfates was limited. The degraded depth was still greater for the AA+SB+AN solution, and is linked to the greater leaching of calcium and silicon, major compounds of the cement matrix.

No exchange mechanism 2 $NH_4^+ \rightarrow Ca^{2+}$ was highlighted since the NH_4^+ concentration was measured and remained constant at about 800 $mg.L^{-1}$ throughout the experiment.

Sodium bicarbonate combined with the other aggressive compounds

In the AA+SB solution, the presence of sodium bicarbonate seems to protect the cement matrix since the amount of leached elements is much smaller and iron and aluminium remain on the surface. The effect of the SB solution is probably associated, at least partially, with an effect on the pH of the AA+SB solution (initial pH of 5.3), significantly greater than that of the AA solution alone (initial pH of 2.6). The mass loss is also lower than for the AA solution but is still significant. Calcium carbonates (calcite and vaterite) were not found on the surface but in depth (zone 3) where the conditions were favourable to precipitation while more of the material was completely decalcified in the surface. Once again, the presence of vaterite in the external carbonated zone was probably linked to a pH<10.

In the AA+AN+SB solution, the lower intensity of the degradation compared to AA+AN solution confirms the protective effect of the sodium bicarbonate. Smaller degraded area and mass loss are observed. The presence of sodium bicarbonate prevents the leaching of aluminium and iron, elements leached only in the presence of acetic acid and in the absence of sodium bicarbonate. In addition, the presence of sodium bicarbonate greatly reduces the amounts of calcium, sulfates and silicon leached out. In this solution, carbonation occurs in depth (zone 3), just before the transition zone containing the sulfur enrichment (zone 2). Its effect on the chemical composition is more significant than in the case of the AA+SB solution. In addition, the presence of sodium bicarbonate in the AA+SB+AN solution induces an initial pH of the solution which is significantly higher (4.9) than for the AA+AN solution (2.4).

4.2 Comparison with real anaerobic digestion liquid media

The previous results can be compared with the study by Giroudon et al. [13] where OPC pastes (water/cement = 0.30) were immersed in the liquid media of anaerobic digestion in bioreactors. In the liquid containing the OPC pastes, the maximum concentrations of aggressive agents encountered were 0.26 $g.L^{-1}$ (4.3 $mmol.L^{-1}$ if only acetic acid is considered) of VFA, 770 $mg.L^{-1}$ of NH_4^+ and about 2000 $mg.L^{-1}$ of inorganic carbon content (or about 20 % of CO_2 in the gas phase). Thus, the materials used are comparable with the present study but the concentration ranges are significantly (VFA and CO_2) or slightly (NH_4^+) higher than the ranges encountered in the study in a real environment. This could be expressed by a higher intensity of degradation.

Figure 7 summarizes the main chemical and mineralogical changes in the OPC pastes exposed to (i) the synthetic AA+SB+AN solution for 16 weeks and (ii) a real anaerobic digestion medium for 17.5 weeks [13], together with exposure conditions and degraded depths. In both studies, the total degradation was expressed by the dissolution of the initial phases (zones 4 and 5), the decalcification of the cementitious matrix associated with a sulfur enrichment and the precipitation of secondary ettringite (zone 2). The presence of dissolved CO_2 led to the carbonation of the paste, with the precipitation of calcite and vaterite (zones 3 and 4).

However, the degradation intensity (altered depth, decalcification, loss of density, mass loss, etc.) was much lower in the real environment since the degraded depth in the AA+SB+AN solution (about 4000 µm from zone 2 to the surface) was about 5 times that in the bioreactors (about 800 µm from zone 2 to the surface), mostly due to the high concentration of acetic acid in the synthetic solutions, and could correspond to real conditions in an industrial digester. Thus, no significant mass loss was detected in the experiment of Giroudon et al. [13], neither was any external amorphous structure. An external amorphous Si-Al gel was, however, identified in studies by Voegel et al. [15,16], where the authors studied the biodeterioration phenomena of cementitious pastes (water/cement = 0.40) in the submerged part of a digester using typical food biowaste. Thus, the degradation intensity is strongly dependent on the evolution of the medium, the type of substrates used and, especially, how the associated process is run. For example, with a rapidly hydrolysable substrate fed continuously using a constant charge, there will be no accumulation of VFA and therefore no pH drop.

In addition, an external phosphorus enrichment has been observed in real media [12,13,15,16], where this element was probably brought by the substrate [16].

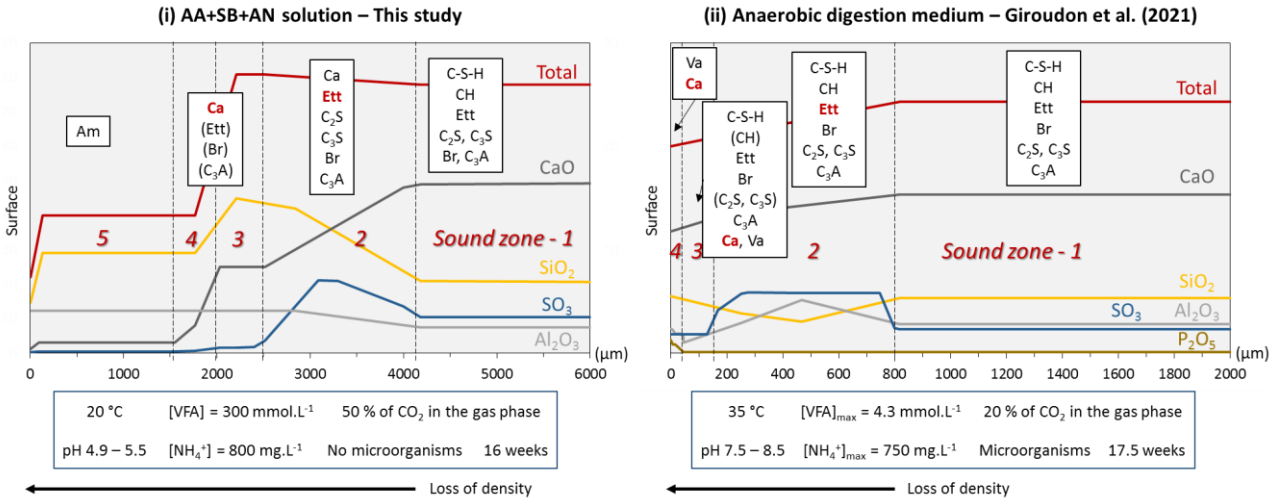

Figure 7: Schematic representations of chemical composition of oxides and mineralogical variations (analysed by EPMA and XRD, respectively) of OPC pastes exposed to (i) a synthetic solution of acetic acid, sodium bicarbonate and ammonium nitrate

for 16 weeks and (ii) a real anaerobic digestion liquid medium for 17.5 weeks [13]. Ett: ettringite; Ca: calcite; Va: vaterite; Br: brownmillerite; Am: mainly amorphous pattern – Red bold characters = intensification of the XRD signal in comparison with the deeper zone; Parentheses = significantly lower intensity of the XRD signal in comparison with the main phase.

4.3 Normative context

In order to quantify the chemical aggressiveness of an environment toward concrete and to design durable structures, the European standard EN 206/CN [26] and the French information document FD P 18-011 [25] classify environments chemically using three classes of increasing aggressiveness: XA1, XA2 and XA3. For this purpose, the concentration and presence of some aggressive agents are taken into account: the aggressive carbon dioxide concentration (aggressive CO_2), the sulfate concentration (SO_4^{2-}), the magnesium ion concentration (Mg^{2+}), the ammonium ion concentration (NH_4^+), the pH, and the water hardness.

According to this study, some inconsistencies can be noted. Whereas both AN and AA solutions are considered to be highly aggressive ($[NH_4^+]>>100$ mg.L^{-1} and pH<<4 for AN and AA solutions respectively), it appears that the AN solution was much less aggressive than the AA solution. Moreover, the AA+SB solution is classified XA2 because of its initial pH (5.32), whereas this solution led to a higher aggressiveness than the AN solution (XA3).

Thus, it might be relevant to consider not only the pH but also the concentration of organic acids in solution, since the pH is not suitable to describe their aggressiveness [38,77]. In addition, recommended cements (such as blast-furnace slag cements) should also be tested.

5 Conclusion

This study assessed the contribution of different aggressive agents to the global degradation of OPC pastes during anaerobic digestion. In the current experimental conditions:

- Despite the different deterioration mechanisms specific to each aggressive agent, the pH plays an important role in the aggressiveness of the solutions studied.
- Immersion in an acetic acid solution led to sharp and total decalcification of the cementitious matrix, with large mass loss and degraded depth. In mixed solutions, acetic acid had a preponderant effect, which led to the total decalcification of the degraded zone, with the appearance of a well-marked structural, mineralogical and chemical zonation.
- The attack by the ammonium nitrate solution expressed itself by a progressive decalcification, with significant mass loss and degraded depth. However, in mixed solution, ammonium nitrate has a negligible effect, even if the concentration used (800 mg.L^{-1}) is much higher than the maximum concentration range considered by standards EN 206 and FD P18-011 for chemically aggressive environments (XA3 class: 60 to 100 mg.L^{-1} of NH_4^+ ion in solution) [25,26].
- By clogging the porosity through carbonation and increasing the pH of the solution though its strong buffering capacity, the sodium bicarbonate solution provides a protective effect when combined with other aggressive agents. However, its effect is not preponderant since the pastes remain highly degraded when acetic acid is present. The significant carbonation in these environments induces a risk of corrosion for reinforced concrete structures.
- While maintaining qualitatively comparable deterioration characteristics, the high concentrations used for the synthetic chemical solutions led to an intensification of the degradation compared to the laboratory environment.
- The normative context does not allow accurate quantification of a solution's aggressiveness for OPC based material, especially in the presence of organic acids.
- Modelling work allowing the pH to be adjusted while various concentrations are being studied would bring new knowledge about the action of each aggressive metabolite on the concrete

attack. Finally, this could also be useful for other structures that house complex biological processes, such as wastewater treatment plants that involve anaerobic digestion, among other treatments [78].

6 Acknowledgements

The authors wish to thank the French National Research Agency (ANR) for its financial support in the project BIBENdOM – ANR – 16 – CE22 – 001 DS0602. The authors also thank Paul Schokmel, Tony Pons and Maud Schiettekatte for their help with the experiment and the analytical support.

7 Supplementary data

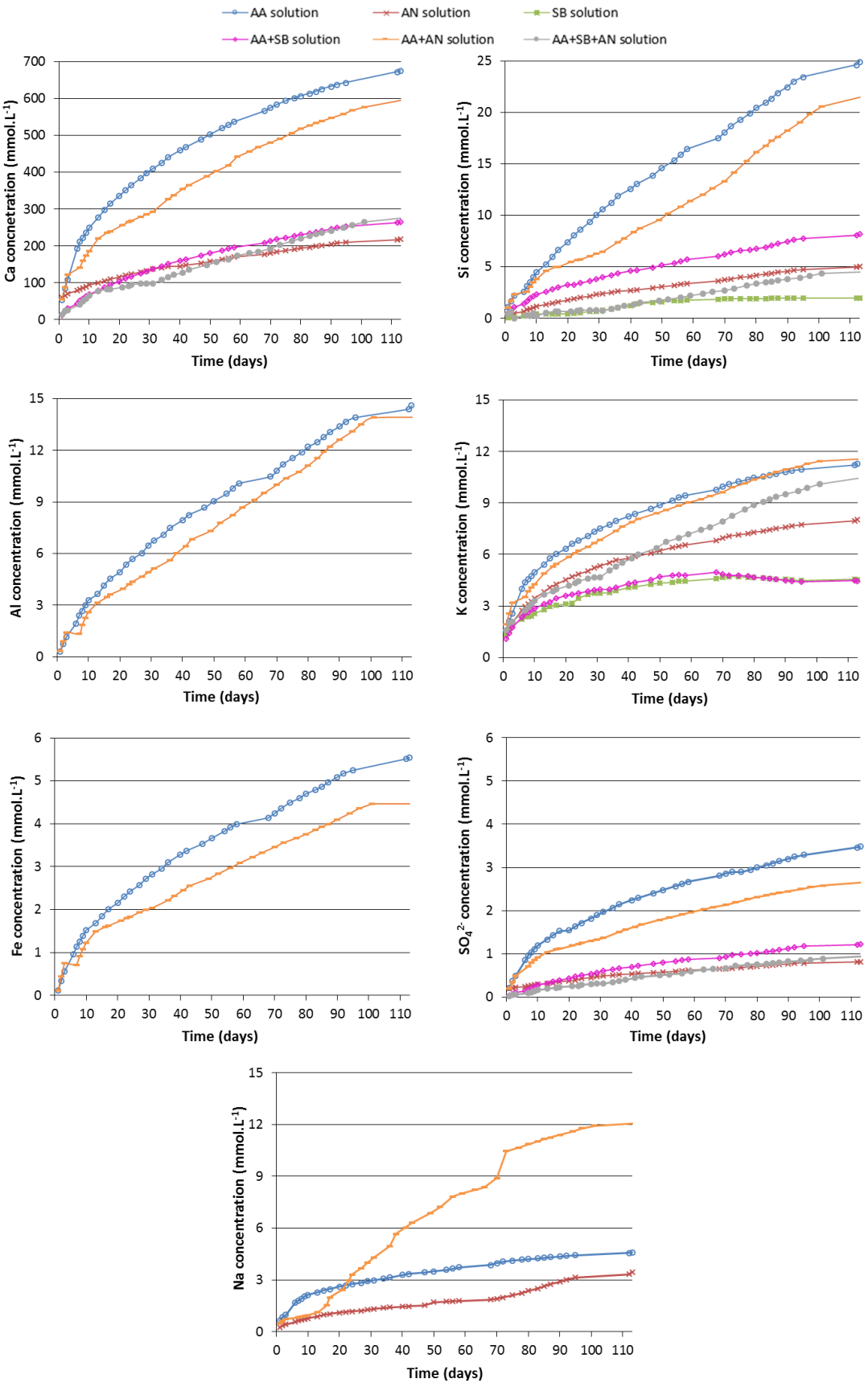

587

588

589 *Appendix A : Cumulated concentrations and leaching kinetics of Ca, Si, Fe, SO_4^{2-}, Al, K, Na*

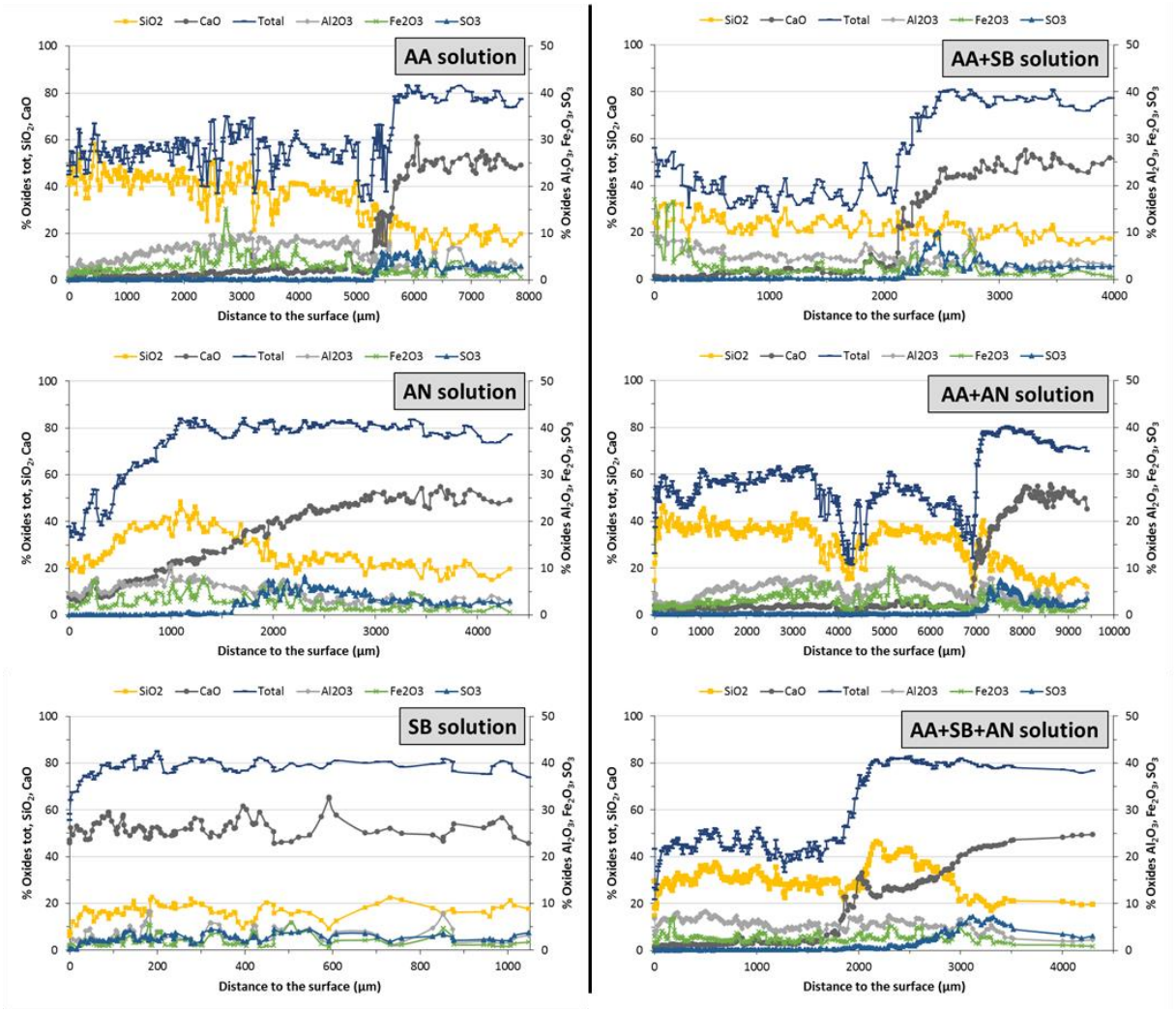

590

591 *Appendix B: Chemical composition profiles of the OPC pastes after 16 weeks of immersion in the aggressive solutions according*
592 *to the distance to the surface*

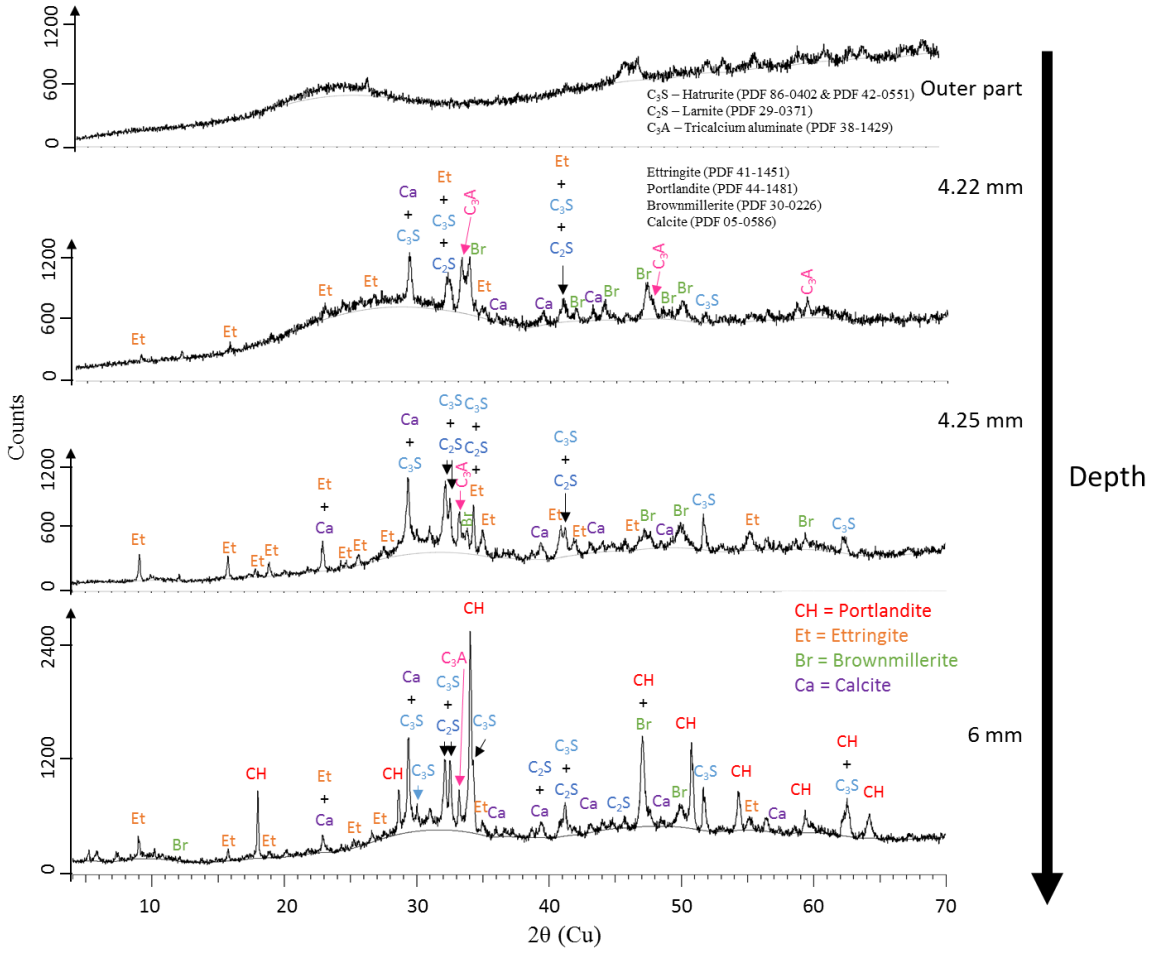

593

594 *Appendix C: X-ray patterns of the OPC specimen immersed in AA solution for 16 weeks according to the depth*

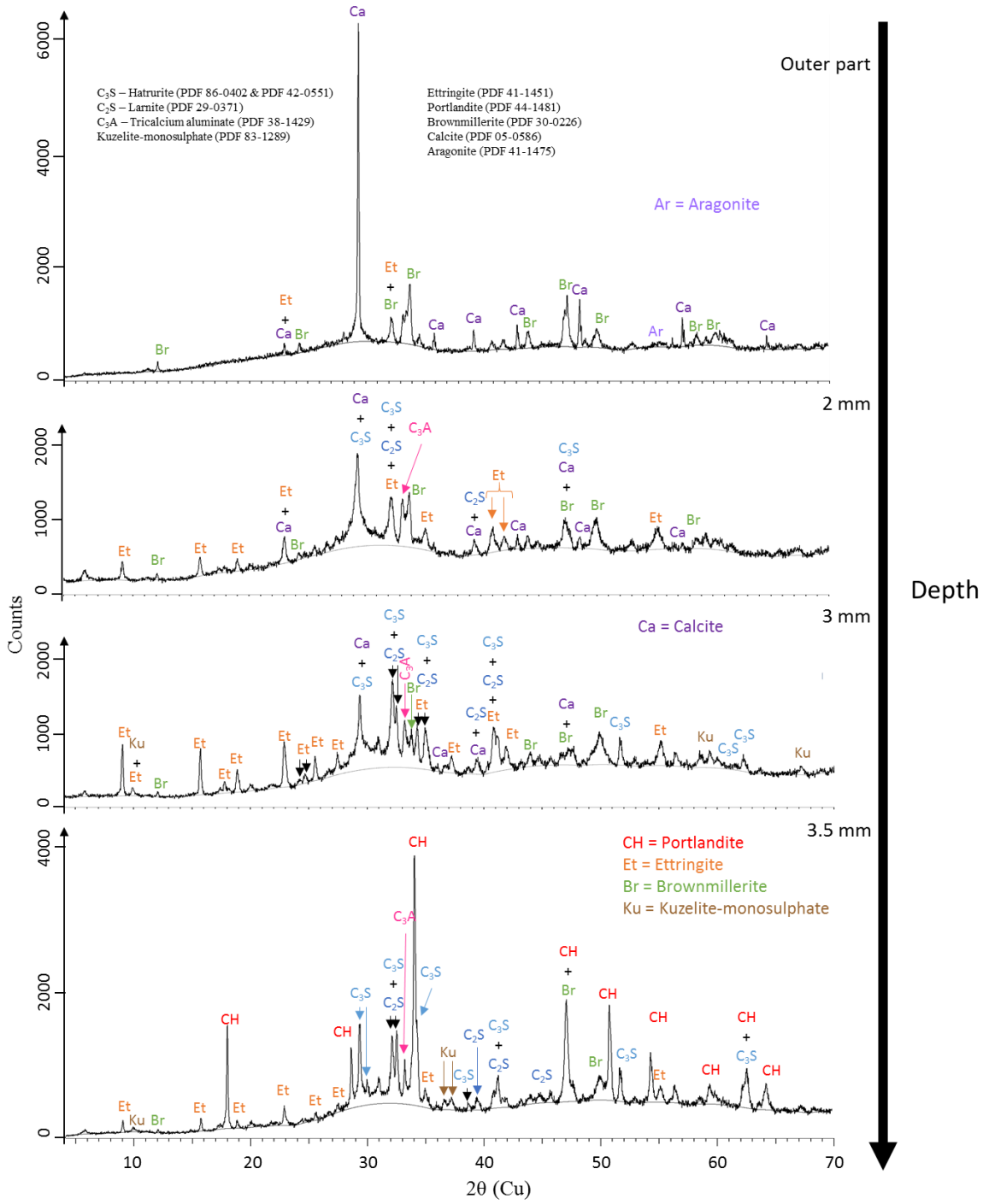

595

596 *Appendix D: X-ray patterns of the OPC specimen immersed in AN solution for 16 weeks according to the depth*

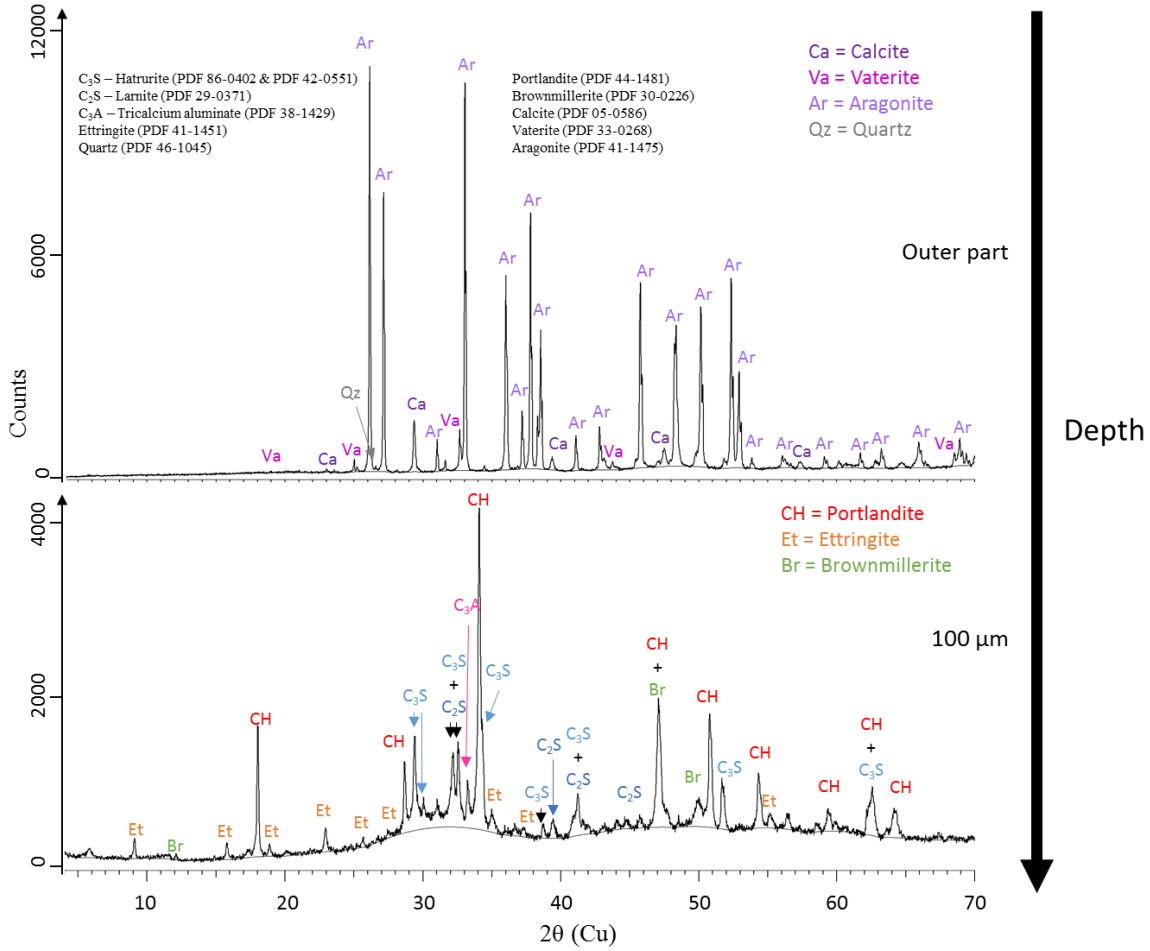

Appendix E: X-ray patterns of the OPC specimen immersed in SB solution for 16 weeks according to the depth

References

[1] G. Lastella, C. Testa, G. Cornacchia, M. Notornicola, F. Voltasio, V.K. Sharma, Anaerobic digestion of semi-solid organic waste: biogas production and its purification, Energy Convers. Manag. 43 (2002) 63–75. https://doi.org/10.1016/S0196-8904(01)00011-5.

[2] M. Lesteur, V. Bellon-Maurel, C. Gonzalez, E. Latrille, J.M. Roger, G. Junqua, J.P. Steyer, Alternative methods for determining anaerobic biodegradability: A review, Process Biochem. 45 (2010) 431–440. https://doi.org/10.1016/j.procbio.2009.11.018.

[3] P. Weiland, Biogas production: current state and perspectives, Appl. Microbiol. Biotechnol. 85 (2010) 849–860. https://doi.org/10.1007/s00253-009-2246-7.

[4] ATEE, Club Biogaz, Statistiques filières biogaz - Juillet 2018, (2018). http://atee.fr/sites/default/files/2018-09-04_statistiques_filiere_biogaz_club_biogaz_vf.pdf (accessed February 7, 2019).

[5] InfoMetha, Etat des lieux de la méthanisation en Europe, InfoMetha. (2020). https://www.infometha.org/effets-socio-economiques/etat-des-lieux-de-la-methanisation-en-europe (accessed September 25, 2020).

[6] H. Fehrenbach, J. Giegrich, G. Reinhardt, U. Sayer, M. Gretz, K. Lanje, J. Schmitz, Kriterien einer nachhaltigen Bioenergienutzung im globalen Ma\s sstab, UBA-Forschungsbericht. 206 (2008) 41–112.

[7] S. Yun, W. Fang, T. Du, X. Hu, X. Huang, X. Li, C. Zhang, P.D. Lund, Use of bio-based carbon materials for improving biogas yield and digestate stability, Energy. 164 (2018) 898–909. https://doi.org/10.1016/j.energy.2018.09.067.

[8] European Biogas Association, Statistical Report of the European Biogas Association Abriged version - 2018, Brussels, 2019.
[9] S. Cole, J.R. Frank, Methane from Biomass: A Systems Approach, Springer Netherlands, 1988.
[10] G.M. Evans, J.C. Furlong, Environmental Biotechnology - Theory and Application, John Wiley & Sons, 2003.
[11] E.S.A. Nathalie Bachmann, 8 - Design and engineering of biogas plants, in: A. Wellinger, J. Murphy, D. Baxter (Eds.), Biogas Handb., Woodhead Publishing, 2013: pp. 191–211. https://doi.org/10.1533/9780857097415.2.191.
[12] A. Bertron, M. Peyre Lavigne, C. Patapy, B. Erable, Biodeterioration of concrete in agricultural, agro-food and biogas plants: state of the art and challenges, RILEM Tech. Lett. 2 (2017) 83–89. https://doi.org/10.21809/rilemtechlett.2017.42.
[13] M. Giroudon, M. Peyre Lavigne, C. Patapy, A. Bertron, Blast-furnace slag cement and metakaolin based geopolymer as construction materials for liquid anaerobic digestion structures: Interactions and biodeterioration mechanisms, Sci. Total Environ. 750 (2021) 141518. https://doi.org/10.1016/j.scitotenv.2020.141518.
[14] A. Koenig, F. Dehn, Biogenic acid attack on concretes in biogas plants, Biosyst. Eng. 147 (2016) 226–237. https://doi.org/10.1016/j.biosystemseng.2016.03.007.
[15] C. Voegel, M. Giroudon, A. Bertron, C. Patapy, M. Peyre Lavigne, T. Verdier, B. Erable, Cementitious materials in biogas systems: Biodeterioration mechanisms and kinetics in CEM I and CAC based materials, Cem. Concr. Res. 124 (2019) 105815. https://doi.org/10.1016/j.cemconres.2019.105815.
[16] C. Voegel, A. Bertron, B. Erable, Mechanisms of cementitious material deterioration in biogas digester, Sci. Total Environ. 571 (2016) 892–901. https://doi.org/10.1016/j.scitotenv.2016.07.072.
[17] H. Fisgativa, A. Tremier, P. Dabert, Characterizing the variability of food waste quality: A need for efficient valorisation through anaerobic digestion, Waste Manag. 50 (2016) 264–274. https://doi.org/10.1016/j.wasman.2016.01.041.
[18] K. Li, R. Liu, C. Sun, Comparison of anaerobic digestion characteristics and kinetics of four livestock manures with different substrate concentrations, Bioresour. Technol. 198 (2015) 133–140. https://doi.org/10.1016/j.biortech.2015.08.151.
[19] A. Bertron, Durabilité des matériaux cimentaires soumis aux acides organiques : cas particulier des effluents d'élevage, Thèse, INSA Toulouse, 2004. http://www.theses.fr/2004ISAT0030.
[20] A. Bertron, J. Duchesne, G. Escadeillas, Degradation of cement pastes by organic acids, Mater. Struct. 40 (2007) 341–354. https://doi.org/10.1617/s11527-006-9110-3.
[21] C. Carde, R. François, J.-M. Torrenti, Leaching of both calcium hydroxide and C-S-H from cement paste: Modeling the mechanical behavior, Cem. Concr. Res. 26 (1996) 1257–1268. https://doi.org/10.1016/0008-8846(96)00095-6.
[22] G. Escadeillas, H. Hornain, La durabilité des bétons vis-à-vis des environnements chimiquement agressifs, in: Durabilité Bétons, Presse de l'ENCP, 2008: pp. 613–705.
[23] C. Gallé, H. Peycelon, P. Le Bescop, Effect of an accelerated chemical degradation on water permeability and pore structure of cement based materials, Adv. Cem. Res. 16 (2004) 105–114. https://doi.org/10.1680/adcr.2004.16.3.105.
[24] F.M. Lea, The action of ammonium salts on concrete, Mag. Concr. Res. 17 (1965) 115–116. https://doi.org/10.1680/macr.1965.17.52.115.
[25] AFNOR, FD P18-011. Concrete - Definition and classification of chemically aggressive environments - Recommendations for concrete mix design, Paris, France, 2016.
[26] AFNOR, NF EN 206/CN. Concrete - Specification, performance, production and conformity - National addition to the standard NF EN 206, Paris, France, 2014.
[27] CIMbéton, Guide de prescription des ciments pour des constructions durables. Cas des bétons coulés en place, 2009. https://www.infociments.fr/ciments/t47-guide-de-prescription-des-ciments-pour-des-constructions-durables (accessed March 1, 2018).

671 [28] CIMbéton, Syndicat National du Béton Prêt à l'Emploi, Syndicat National du Pompage du Béton,
672 Institut de l'Elevage, Ouvrages en béton pour l'exploitation agricole et les aménagements ruraux
673 - Conception, prescription, réalisations, CIMbéton, 2007.
674 https://www.infociments.fr/sites/default/files/article/fichier/CT-B66.pdf (accessed February 28,
675 2018).
676 [29] P.H.R. Borges, J.O. Costa, N.B. Milestone, C.J. Lynsdale, R.E. Streatfield, Carbonation of CH and
677 C–S–H in composite cement pastes containing high amounts of BFS, Cem. Concr. Res. 40 (2010)
678 284–292. https://doi.org/10.1016/j.cemconres.2009.10.020.
679 [30] V.T. Ngala, C.L. Page, Effects of carbonation on pore structure and diffusional properties of
680 hydrated cement pastes, Cem. Concr. Res. 27 (1997) 995–1007. https://doi.org/10.1016/S0008-
681 8846(97)00102-6.
682 [31] B. Šavija, M. Luković, Carbonation of cement paste: Understanding, challenges, and
683 opportunities, Constr. Build. Mater. 117 (2016) 285–301.
684 https://doi.org/10.1016/j.conbuildmat.2016.04.138.
685 [32] E. Gruyaert, P. Van den Heede, M. Maes, N. De Belie, Investigation of the influence of blast-
686 furnace slag on the resistance of concrete against organic acid or sulphate attack by means of
687 accelerated degradation tests, Cem. Concr. Res. 42 (2012) 173–185.
688 https://doi.org/10.1016/j.cemconres.2011.09.009.
689 [33] O. Oueslati, J. Duchesne, The effect of SCMs and curing time on resistance of mortars subjected
690 to organic acids, Cem. Concr. Res. 42 (2012) 205–214.
691 https://doi.org/10.1016/j.cemconres.2011.09.017.
692 [34] A. Bertron, J. Duchesne, G. Escadeillas, Attack of cement pastes exposed to organic acids in
693 manure, Cem. Concr. Compos. 27 (2005) 898–909.
694 https://doi.org/10.1016/j.cemconcomp.2005.06.003.
695 [35] AFNOR, NF EN 196-1. Methods of testing cement - Part 1: Determination of strength, Paris,
696 France, 2016.
697 [36] AFNOR, NF P18-459. Concrete - Testing hardened concrete - Testing porosity and density, Paris,
698 France, 2010.
699 [37] A. Bertron, J. Duchesne, Attack of Cementitious Materials by Organic Acids in Agricultural and
700 Agrofood Effluents, in: Perform. Cem.-Based Mater. Aggress. Aqueous Environ., Springer,
701 Dordrecht, 2013: pp. 131–173. https://doi.org/10.1007/978-94-007-5413-3_6.
702 [38] S. Larreur-Cayol, A. Bertron, G. Escadeillas, Degradation of cement-based materials by various
703 organic acids in agro-industrial waste-waters, Cem. Concr. Res. 41 (2011) 882–892.
704 https://doi.org/10.1016/j.cemconres.2011.04.007.
705 [39] D.T. Hill, R.D. Holmberg, Long chain volatile fatty acid relationships in anaerobic digestion of
706 swine waste, Biol. Wastes. 23 (1988) 195–214. https://doi.org/10.1016/0269-7483(88)90034-1.
707 [40] W. Parawira, M. Murto, J.S. Read, B. Mattiasson, Volatile fatty acid production during anaerobic
708 mesophilic digestion of solid potato waste, J. Chem. Technol. Biotechnol. 79 (2004) 673–677.
709 https://doi.org/10.1002/jctb.1012.
710 [41] E.R. Viéitez, S. Ghosh, Biogasification of solid wastes by two-phase anaerobic fermentation,
711 Biomass Bioenergy. 16 (1999) 299–309. https://doi.org/10.1016/S0961-9534(99)00002-1.
712 [42] C. Voegel, A. Bertron, B. Erable, Microbially induced degradation of cement-based materials in
713 biogas production industrial process, in: Sao Paulo, 2014.
714 [43] O.P. Karthikeyan, C. Visvanathan, Bio-energy recovery from high-solid organic substrates by dry
715 anaerobic bio-conversion processes: a review, Rev. Environ. Sci. Biotechnol. 12 (2013) 257–284.
716 https://doi.org/10.1007/s11157-012-9304-9.
717 [44] O. Yenigün, B. Demirel, Ammonia inhibition in anaerobic digestion: A review, Process Biochem.
718 48 (2013) 901–911. https://doi.org/10.1016/j.procbio.2013.04.012.
719 [45] D. Deublein, A. Steinhauser, Biogas from Waste and Renewable Resources: An Introduction, John
720 Wiley & Sons, 2011.

[46] S. Rasi, Biogas composition and upgrading to biomethane, Jyväskylä studies in Biological and Environmental Science, University of Jyväskylä, 2009. https://jyx.jyu.fi/handle/123456789/20353 (accessed April 8, 2020).
[47] S. Rasi, A. Veijanen, J. Rintala, Trace compounds of biogas from different biogas production plants, Energy. 32 (2007) 1375–1380. https://doi.org/10.1016/j.energy.2006.10.018.
[48] A. Bertron, J. Duchesne, G. Escadeillas, Accelerated tests of hardened cement pastes alteration by organic acids: analysis of the pH effect, Cem. Concr. Res. 35 (2005) 155–166. https://doi.org/10.1016/j.cemconres.2004.09.009.
[49] V. Pavlík, Corrosion of hardened cement paste by acetic and nitric acids part II: Formation and chemical composition of the corrosion products layer, Cem. Concr. Res. 24 (1994) 1495–1508. https://doi.org/10.1016/0008-8846(94)90164-3.
[50] G. Escadeillas, Ammonium Nitrate Attack on Cementitious Materials, in: Perform. Cem.-Based Mater. Aggress. Aqueous Environ., Springer, Dordrecht, 2013: pp. 113–130. https://doi.org/10.1007/978-94-007-5413-3_5.
[51] C. Carde, G. Escadeillas, R. François, Use of ammonium nitrate solution to simulate and accelerate the leaching of cement pastes due to deionized water, Mag. Concr. Res. 49 (1997) 295–301.
[52] C. Carde, R. François, Effect of the leaching of calcium hydroxide from cement paste on mechanical and physical properties, Cem. Concr. Res. 27 (1997) 539–550. https://doi.org/10.1016/S0008-8846(97)00042-2.
[53] C. Perlot, X. Bourbon, M. Carcasses, G. Ballivy, The adaptation of an experimental protocol to the durability of cement engineered barriers for nuclear waste storage, Mag. Concr. Res. 59 (2007) 311–322. https://doi.org/10.1680/macr.2007.59.5.311.
[54] B. Gérard, C. Le Bellego, O. Bernard, Simplified modelling of calcium leaching of concrete in various environments, Mater. Struct. 35 (2002) 632–640. https://doi.org/10.1007/BF02480356.
[55] F.H. Heukamp, F.-J. Ulm, J.T. Germaine, Mechanical properties of calcium-leached cement pastes: Triaxial stress states and the influence of the pore pressures, Cem. Concr. Res. 31 (2001) 767–774. https://doi.org/10.1016/S0008-8846(01)00472-0.
[56] K. Wan, Y. Li, W. Sun, Experimental and modelling research of the accelerated calcium leaching of cement paste in ammonium nitrate solution, Constr. Build. Mater. 40 (2013) 832–846. https://doi.org/10.1016/j.conbuildmat.2012.11.066.
[57] K. Kurumisawa, K. Haga, D. Hayashi, H. Owada, Effects of calcium leaching on diffusion properties of hardened and altered cement pastes, Phys. Chem. Earth Parts ABC. 99 (2017) 175–183. https://doi.org/10.1016/j.pce.2017.03.007.
[58] K. Kurumisawa, T. Nawa, H. Owada, M. Shibata, Deteriorated hardened cement paste structure analyzed by XPS and 29Si NMR techniques, Cem. Concr. Res. 52 (2013) 190–195. https://doi.org/10.1016/j.cemconres.2013.07.003.
[59] V. Baroghel-Bouny, B. Capra, D. Laurens, La durabilité des armatures et du béton d'enrobage, in: Durabilité Bétons, Presse de l'ENCP, 2008: pp. 303–385.
[60] V. Shah, K. Scrivener, B. Bhattacharjee, S. Bishnoi, Changes in microstructure characteristics of cement paste on carbonation, Cem. Concr. Res. 109 (2018) 184–197. https://doi.org/10.1016/j.cemconres.2018.04.016.
[61] S. Knez, D. Klinar, J. Golob, Stabilization of PCC dispersions prepared directly in the mother-liquid after synthesis through the carbonation of (hydrated) lime, Chem. Eng. Sci. 61 (2006) 5867–5880. https://doi.org/10.1016/j.ces.2006.05.016.
[62] A. Morandeau, Carbonatation atmosphérique des systèmes cimentaires à faible teneur en portlandite, Thèse, Paris Est, 2013. http://www.theses.fr/2013PEST1032 (accessed April 10, 2019).
[63] K. Sawada, The mechanisms of crystallization and transformation of calcium carbonates, Pure Appl. Chem. 69 (1997) 921–928. https://doi.org/10.1351/ pac199769050921.
[64] P. Cailleau, C. Jacquin, D. Dragone, A. Girou, H. Roques, L. Humbert, Influence des ions étrangers et de la matière organique sur la cristallisation des carbonates de calcium, Rev. Inst. Fr. Pétrole. 34 (1979) 83–112. https://doi.org/10.2516/ogst:1979003.

[65] H. El Fil, Contribution à l'étude des eaux géothermales du sud tunisien : étude des mécanismes et de la prévention des phénomènes d'entartrage, Thèse, INSA Toulouse, 1999. http://www.theses.fr/1999ISAT0002 (accessed June 20, 2019).
[66] M. Zidoune, Contribution à la connaissance des mécanismes d'entartrage par diverses méthodes électrochimiques, Thèse, Paris 6, 1996. http://www.theses.fr/1996PA066445 (accessed June 20, 2019).
[67] O.A. Jimoh, K.S. Ariffin, H.B. Hussin, A.E. Temitope, Synthesis of precipitated calcium carbonate: a review, Carbonates Evaporites. 33 (2018) 331–346. https://doi.org/10.1007/s13146-017-0341-x.
[68] M. Kitamura, H. Konno, A. Yasui, H. Masuoka, Controlling factors and mechanism of reactive crystallization of calcium carbonate polymorphs from calcium hydroxide suspensions, J. Cryst. Growth. 236 (2002) 323–332. https://doi.org/10.1016/S0022-0248(01)02082-6.
[69] Ç.M. Oral, B. Ercan, Influence of pH on morphology, size and polymorph of room temperature synthesized calcium carbonate particles, Powder Technol. 339 (2018) 781–788. https://doi.org/10.1016/j.powtec.2018.08.066.
[70] C.Y. Tai, F.-B. Chen, Polymorphism of CaCO3, precipitated in a constant-composition environment, AIChE J. 44 (1998) 1790–1798. https://doi.org/10.1002/aic.690440810.
[71] C. Chalhoub, R. François, M. Carcasses, Effect of Cathode–Anode distance and electrical resistivity on macrocell corrosion currents and cathodic response in cases of chloride induced corrosion in reinforced concrete structures, Constr. Build. Mater. 245 (2020) 118337. https://doi.org/10.1016/j.conbuildmat.2020.118337.
[72] N. Li, N. Farzadnia, C. Shi, Microstructural changes in alkali-activated slag mortars induced by accelerated carbonation, Cem. Concr. Res. 100 (2017) 214–226. https://doi.org/10.1016/j.cemconres.2017.07.008.
[73] M. Nedeljković, B. Šavija, Y. Zuo, M. Luković, G. Ye, Effect of natural carbonation on the pore structure and elastic modulus of the alkali-activated fly ash and slag pastes, Constr. Build. Mater. 161 (2018) 687–704. https://doi.org/10.1016/j.conbuildmat.2017.12.005.
[74] F. Puertas, M. Palacios, T. Vázquez, Carbonation process of alkali-activated slag mortars, J. Mater. Sci. 41 (2006) 3071–3082. https://doi.org/10.1007/s10853-005-1821-2.
[75] M.Á. Sanjuán, E. Estévez, C. Argiz, D. del Barrio, Effect of curing time on granulated blast-furnace slag cement mortars carbonation, Cem. Concr. Compos. 90 (2018) 257–265. https://doi.org/10.1016/j.cemconcomp.2018.04.006.
[76] S. Poyet, P.L. Bescop, M. Pierre, L. Chomat, C. Blanc, Accelerated leaching of cementitious materials using ammonium nitrate (6M): influence of test conditions, Eur. J. Environ. Civ. Eng. (2012). https://www.tandfonline.com/doi/pdf/10.1080/19648189.2012.667712?needAccess=true&redirect=1 (accessed May 15, 2020).
[77] A. Bertron, Understanding interactions between cementitious materials and microorganisms: a key to sustainable and safe concrete structures in various contexts, Mater. Struct. 47 (2014) 1787–1806. https://doi.org/10.1617/s11527-014-0433-1.
[78] C. Gallert, J. Winter, Bacterial Metabolism in Wastewater Treatment Systems, in: H.-J. Jördening, J. Winter (Eds.), Environ. Biotechnol. - Concept Appl., 1st ed., John Wiley & Sons, Ltd, 2005. https://doi.org/10.1002/3527604286.

818